Long-Range Photoinduced Through-Bond Electron Transfer and Radiative Recombination via Rigid Nonconjugated Bridges: Distance and Solvent Dependence[1]

Henk Oevering,[†] Michael N. Paddon-Row,*[‡] Marc Heppener,[†] Anna M. Oliver,[‡] E. Cotsaris,[‡] Jan W. Verhoeven,*[†] and Noel S. Hush[§]

Contribution from the Laboratory of Organic Chemistry and the Laboratory of Physical Chemistry, University of Amsterdam, Nieuwe Achtergracht 129, 1018 WS Amsterdam, The Netherlands, the Department of Chemistry, University of New South Wales, Kensington, N.S.W. 2033, Australia, and the Department of Theoretical Chemistry, University of Sydney, Sydney, N.S.W. 2006, Australia. *Received October 20, 1986*

Abstract: A series of molecules **1** was synthesized containing a 1,4-dimethoxynaphthalene donor (D) and a 1,1-dicyanoethylene acceptor (A) interconnected by five different, rigid, nonconjugated bridges. The length of the bridges varies with increments of two σ-bonds from four in **1(4)** to 12 σ-bonds in **1(12)**, to provide donor–acceptor center-to-center separations (R_c) ranging from 7.0–14.9 Å. In solvents of medium and high polarity, excitation of the donor D is followed by rapid intramolecular electron transfer. The rate constant (k_{et}) shows only small dependence upon the solvent polarity (a factor of 2–3 between benzene and acetonitrile, for example) but decreases with increasing separation ranging from $>10^{11}$ s^{-1} for a four-bond separation to $\approx 4 \times 10^8$ s^{-1} for a 12-bond separation. In saturated hydrocarbon solvents photoinduced electron transfer is not observed for 10- and 12-bond separations, while it is not significantly decreased for the shorter homologues. Therefore the absence of electron transfer at 10- and 12-bond separations in saturated hydrocarbon solvents is attributed to a thermodynamic rather than to a kinetic effect. In solvents where electron transfer is thermodynamically feasible, its rate is considerably greater than that found from various other experimental studies where either different bridges were used or intermolecular electron transfer was studied. Through-bond interaction involving σ/π interaction between the bridge and the donor–acceptor pair is proposed to explain the very high electron transfer rates observed in **1**; this is qualitatively correlated with independent information about this coupling derived from both theory and experiment (photoelectron spectroscopy). The observation of intramolecular charge-transfer absorption and emission for **1(4)**, **1(6)**, and **1(8)** confirms the operation of such through-bond interaction. Rigid systems like **1** can therefore not only provide more insight into the thermodynamics of electron transfer and its solvent dependence but especially also into the role of the nature of the coupling of donor and acceptor. The latter is of crucial importance for a better understanding of the factors governing the rates of electron transfer between redox centers in, e.g., biologically important redox proteins involved in photosynthesis and in the respiratory cycle. It is shown that the near-independence of the photoassisted charge separation dynamics on solvent polarity and the overall free-energy change (even for a calculated variation of ~0.9 eV) is consistent with predictions of electron-transfer theory on the assumption that the solvent is a continuous dielectric. It is also shown how the parameters entering into the theoretical expressions (in particular, the intramolecular reorganization energy) may be correlated with those obtained from radiative transitions (e.g., charge recombination fluorescence). The dependence of the effective electron interaction element (J), which couples donor and acceptor, on the bridge length is discussed.

Single electron transfer constitutes one of the most fundamental chemical reactions and plays a crucial role in many synthetic as well as biological processes, occurring under either thermal[2] or under photochemical[3] conditions.

Various lines of experimental evidence have led to the conclusion that both thermal[2] and photoinduced[1,4-8] electron transfer may occur between species separated by a distance significantly exceeding the sum of their van der Waals radii. In fact many biological electron transport processes—including the primary steps of photosynthesis[9]—involve such long-range electron-transfer events. Biological and modified biological systems containing a variety of redox centers at widely different distances, between which electron transfer occurs on a time scale extending from the picosecond regime to many seconds, have been studied.[10-20] Systematic variation of donor and acceptor at a single rigidly fixed distance has recently been used[15,21-23] to establish the dependence of the rate of electron transfer upon the thermodynamic driving force. These studies corroborated earlier theoretical predictions of the existence of an optimal rate constant. In addition, significant progress has been made in the study of the distance dependence of electron transfer especially by measuring the time resolved evolution of the number of electron-transfer events in dilute rigid solutions containing donor and acceptor species.[2] The evaluation of such measurements, however, rests inter alia on the assumption of a statistical distribution of donor–acceptor distances and relative orientations. Consequently no information about specific orientational effects can be found, and furthermore the requirement

[†] University of Amsterdam.
[‡] University of New South Wales.
[§] University of Sydney.

(1) For earlier communications in this series, see: (a) Hush, N. S.; Paddon-Row, M. N.; Cotsaris, E.; Oevering, H.; Verhoeven, J. W.; Heppener, M. *Chem. Phys. Lett.* **1985**, *117*, 8-11. (b) Warman, J. M.; de Haas, M. P.; Paddon-Row, M. N.; Cotsaris, E.; Hush, N. S.; Oevering, H.; Verhoeven, J. W. *Nature* (London) **1986**, *320*, 615-616. (c) Warman, J. M.; de Haas, M. P.; Oevering, H.; Verhoeven, J. W.; Paddon-Row, M. N.; Oliver, A. M.; Hush, N. S. *Chem. Phys. Lett* **1986**, *128*, 95-99. (d) Verhoeven, J. W.; Paddon-Row, M. N.; Hush, N. S.; Oevering, H.; Heppener, M. *Pure Appl. Chem.* **1986**, *58*, 1285-1290.

(2) Miller, J. R.; Beitz, J. V.; Huddleston, R. K. *J. Am. Chem. Soc.* **1984**, *106*, 5057-5068, and references cited therein.

(3) For a recent review on photoinduced electron-transfer see: Creed, D.; Caldwell, R. A. *Photochem. Photobiol.* **1985**, *180*, 715-739.

(4) Kuhn, H. *J. Photochem.* **1979**, *10*, 111-132.

(5) Mobius, D. *Ber. Bunsenges. Phys. Chem.* **1978**, *82*, 848-858.

(6) Pasman, P.; Verhoeven, J. W.; de Boer, Th. *J. Chem. Phys. Lett.* **1978**, *59*, 381-385.

(7) Pasman, P.; Koper, N. W.; Verhoeven, J. W. *Recl. Trav. Chim. Pays-Bas* **1982**, *101*, 363-364.

(8) Li, T. T. T.; Weaver, M. J. *J Am. Chem. Soc* **1984**, *106*, 6107-6108.

(9) Deisenhofer, J.; Epp, O.; Miki, K.; Huber, R.; Michel, H. *J. Mol. Biol.* **1984**, *180*, 385-398.

(10) Isied, S. S.; Worosila, G.; Atherton, S. J. *J. Am. Chem. Soc.* **1982**, *104*, 7659-7661.

(11) Winkler, J.; Nocera, D.; Yocum, K.; Bordignon, E.; Gray, H. B. *J. Am. Chem. Soc.* **1982**, *104*, 5798-5800.

(12) McLendon, G.; Winkler, J.; Nocera, D.; Mauk, A. G.; Gray, H. B. *J. Am. Chem. Soc.* **1985**, *107*, 739-740.

(13) McGourty, J.; Blough, N.; Hoffman, B. *J. Am. Chem. Soc.* **1983**, *105*, 4470-4472.

(14) Isied, S. S.; Kuehn, C.; Worosila, G. *J. Am. Chem. Soc.* **1984**, *106*, 1722-1726.

0002-7863/87/1509-3258$01.50/0

Scheme I. Survey of Synthetic Routes

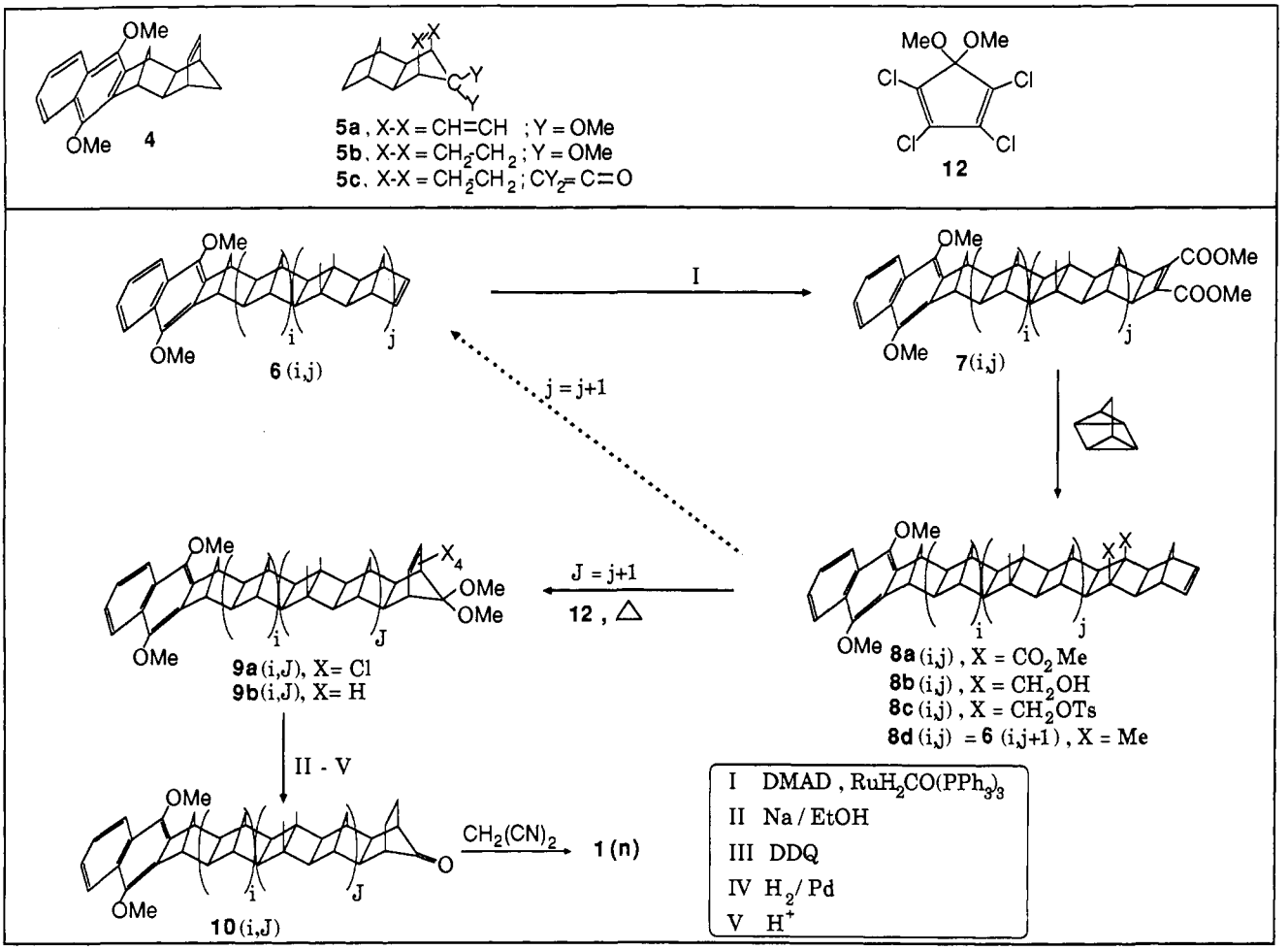

of working in a rigid matrix largely abolishes the possibility of studying the effect of solvation dynamics on the rate of electron transfer. In several recent studies[20,22,24] the latter problem was avoided by introducing "spacers" that maintain a reasonably well-defined donor–acceptor distance but still allow for much rotational freedom. We have therefore embarked[1,25] on the study of series of molecules containing a single electron donor–acceptor pair in a rigidly defined relative orientation and at a rigidly defined distance, the latter being varied in discrete steps throughout the series. The present paper describes the synthesis and the results of measurements of the rate of photoinduced, intramolecular electron transfer for such a series (**1**(*n*), n = 4, 6, 8, 10, 12, cf. Figure 1). These molecules incorporate a 1,4-dimethoxynaphthalene group as the photoexcitable electron donor and a 1,1-dicyanoethylene group as an electron acceptor, the minimum number of carbon–carbon σ-bonds separating these groups being n. In addition, spectroscopic measurements of charge-transfer recombination fluorescence and absorption have been made that yield valuable insight into the reaction mechanism. Molecules **2** and **3** (see Figure 1) will be used as models to study the properties of the isolated donor and acceptor systems.

In Figure 1 the center-to-center distance (R_c) between the donor and acceptor moieties has been indicated as measured from the midpoint of the central C–C bond of the naphthalene system to the central C-atom of the acceptor. In addition Figure 1 compiles the edge-to-edge distances (R_e) between the bond that the donor shares with the bridge and the C-atom that the acceptor shares with the bridge. In estimating these distances, account has been taken of the slight curvature of the bridges as revealed by X-ray structure analysis of **1**(**6**) and of the ketone precursors of **1**(**8**) and **1**(**10**).

Results and Discussion

Syntheses. The generalized synthetic strategy for compounds **1** is outlined in Scheme I. In discussing the synthetic strategy followed it is convenient to refer to a structure in terms of two numbers, i and j, which specify respectively the number of cyclopentyl and tricyclo[4.3.0.0^{2,5}] repeating units. Thus, **6**(**1,1**) refers to structure **6** in which the naphthalene and double bond chromophores are separated by eight σ-bonds. The compounds **1** can be classified into two sets: those in which the chromophores are separated by 4p σ-bonds (p = 1, 2, etc.), such as **1**(**4**), **1**(**8**), and **1**(**12**), and those which contain (4p + 2) σ-bonds, i.e., **1**(**6**) and **1**(**10**). The 4p and 4p + 2 sets of compounds can be synthesized from the respective sets of monoenes, **6**(**0,p-1**) and **6**-(**1,p-1**). The monoenes are readily available through a homologation process[26,27] which is shown in Scheme I. The RuH_2CO-

(15) McLendon, G.; Miller, J. R. *J. Am. Chem. Soc.* **1985**, *107*, 7811–7816.
(16) Isied, S. S.; Vassilian, A.; Magnuson, R. H.; Schwarz, H. A. *J. Am. Chem. Soc.* **1985**, *107*, 7432–7438.
(17) Gust, D.; Moore, T. A. *J. Photochem.* **1985**, *29*, 173–184.
(18) Schmidt, J. A.; Siemiarczuk, A.; Weedon, A. C.; Bolton, J. R. *J. Am. Chem. Soc.* **1985**, *107*, 6112–6114.
(19) Wasielewski, M. R.; Niemczyk, M. P.; Svec, W. A.; Bradley-Pewitt, E. *J. Am. Chem. Soc.* **1985**, *107*, 5562–5563.
(20) Joran, A. D.; Leland, A.; Geller, G. G.; Hopfield, J. J.; Dervan, P. B. *J. Am. Chem. Soc.* **1984**, *106*, 6090–6092.
(21) Miller, J. R.; Calcaterra, L. T.; Closs, G. L. *J. Am. Chem. Soc.* **1984**, *106*, 3047–3049.
(22) Closs, G. L.; Calcaterra, L. T.; Green, N. J.; Penfield, K. W.; Miller, J. R. *J. Phys. Chem.* **1986**, *90*, 3673–3683.
(23) Wasielewski, M. R.; Niemczyk, M. D.; Svec, W. A.; Pewitt, E. B. *J. Am. Chem. Soc.* **1985**, *107*, 1080–1082.
(24) Heitele, H.; Michel-Beyerle, M. E. *J. Am. Chem. Soc.* **1985**, *107*, 8286–8288.
(25) Pasman, P.; Mes, G. F.; Koper, N. W.; Verhoeven, J. W. *J. Am. Chem. Soc.* **1985**, *107*, 5839–5843.

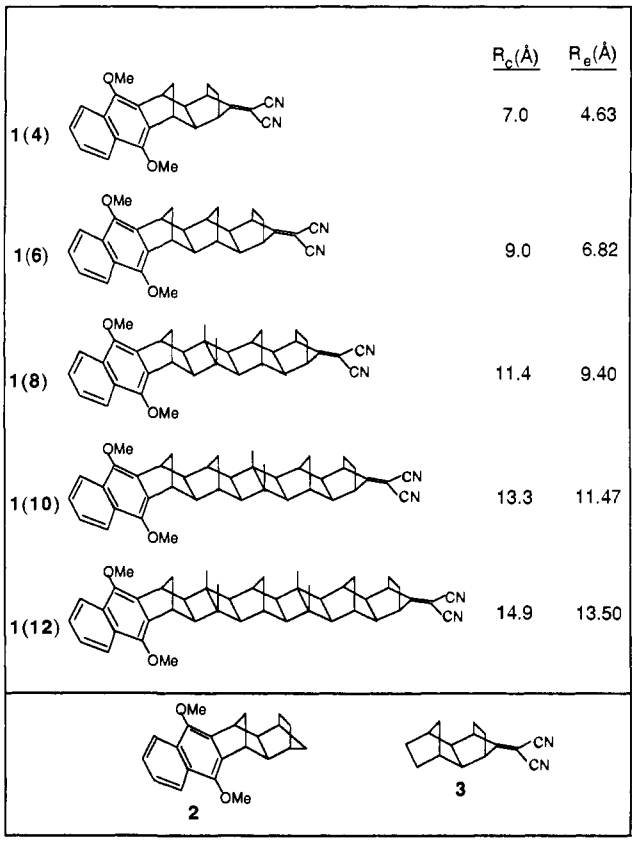

Figure 1. Structure of bridged donor–acceptor molecules (**1**(*n*), *n* = 4, 6, 8, 10, 12) and model systems (**2**,**3**) studied. R_e and R_c give the edge-to-edge and center-to-center distance, respectively, between donor and acceptor.

$(PPh_3)_3$ catalyzed[28] (2 + 2) cycloaddition of dimethylacetylenedicarboxylate (DMAD) to **6**(*i*,*j*) gives the adduct **7**(*i*,*j*). This compound undergoes the expected[26,27,29,30] (2 + 2 + 2) thermal cycloaddition reaction with quadricyclane to give **8a**(*i*,*j*). Conversion of this adduct to **8d**(*i*,*j*+**1**) (= **8**(*i*,*J*)) is readily achieved through the diol, **8b**(*i*,*j*), and $LiAlH_4$ reduction of the bismesylate derivative **8c**(*i*,*j*) formed therefrom. Thus the original monoene has been homologated by four σ-bonds. In this way all higher members of the monoenes can be synthesized, from either **6**(**0**,**0**)[31] or **6**(**1**,**0**).[27] Diels–Alder cycloaddition of the corresponding monoene to dimethoxytetrachlorocyclopentadiene **12** gave the adduct **9a**(*i*,*J*). This adduct can be reductively dehalogenated, to give **9b**(*i*,*J*), through treatment with Na/EtOH. However, this led to a mixture of products formed from partial reduction of the naphthalene ring. Rearomatization was achieved through treatment of the mixture with DDQ. Catalytic hydrogenation followed by deacetalization gave the ketone **10**(*i*,*J*), which is easily converted to the corresponding dicyanomethylene compound **1** by using standard methods (see Experimental Section).

Thermodynamics of Photoinduced Electron Transfer. The free-energy change for photoinduced electron transfer (1) between an excited donor molecule (D*) and a ground-state acceptor molecule at a separation R_c is written as $\Delta G(R_c)$,

$$D^* + A \rightarrow D^+ + A^- \qquad \Delta G(R_c) \qquad (1)$$

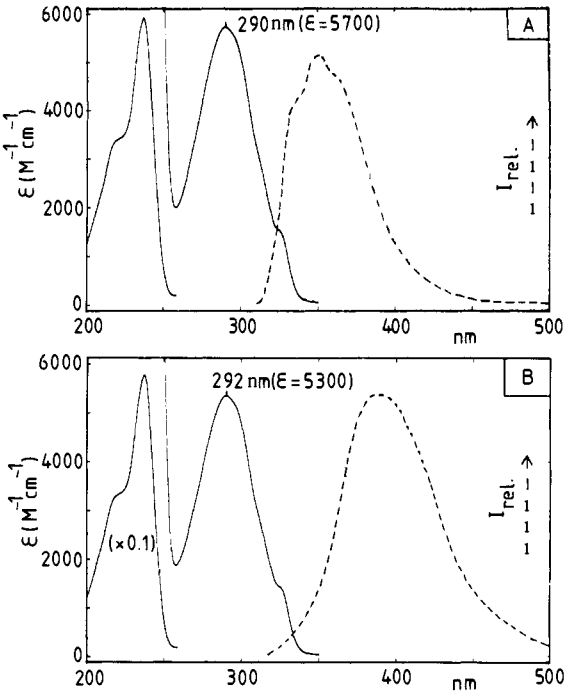

Figure 2. Absorption (—) and emission (- - -) spectra of **2** in cyclohexane (A) and acetonitrile (B).

Table I. Emission Data for Donor **2** in Various Solvents

solvent	λ_{max} (nm)	ϕ	τ (ns)
cyclohexane	350	0.35	5.43
benzene	368	0.33	4.13
di-*n*-butyl ether	354	0.33	4.78
diethyl ether	357	0.27	4.82
ethyl acetate	368	0.40	4.39
tetrahydrofuran	370	0.24	4.26
acetonitrile	386	0.33	4.78

For the present systems at infinite separation we set this equal to (2)

$$\Delta G(\infty) = -E_{00}(\mathbf{2}) + F(E_{ox}(\mathbf{2}) - E_{red}(\mathbf{3})) \qquad (2)$$

In (2) $E_{00}(\mathbf{2})$ is the energy of the zero–zero transition to the lowest excited singlet state (represented by D*) of the donor model system **2**, and $E_{ox}(\mathbf{2})$ and $E_{red}(\mathbf{3})$ are respectively the first one-electron oxidation potential of **2** and the first one-electron reduction potential of the acceptor **3** in the solvent under consideration.

Electrochemical measurements were made for **2** and **3** in acetonitrile solution at a glassy carbon electron (see Experimental Section). The value $E_{ox}(\mathbf{2})$ is +1.1 ± 0.03 V vs. SCE; the cyclic voltammogram indicates reversible formation of a radical cation. The value of $E_{red}(\mathbf{3})$ is more approximate, as formation of the radical anion is found to be largely irreversible in this solvent, indicating that secondary reactions are significant on the time scale of the electrochemical experiments. Under these circumstances the apparent redox potential is shifted anodically with respect to the actual reversible value and furthermore becomes a function of the scan rate. It has been shown,[34] however, that the deviation hardly exceeds 0.1 V, and therefore a value $E_{red}(\mathbf{3}) = -1.7$ to -1.8 V vs. SCE was deduced via $E_{red} = E_{pc} + 0.03$, where E_{pc} represents the cathodic peak potential. This is close to that (−1.69 V) reported earlier for a similar system.[35]

The energy of the lowest singlet excited state of the electron donor **2** and acceptor **3** has been determined from a study of the electronic absorption and fluorescence emission spectra. Relevant spectra of **2** are shown in Figure 2. In addition, the energies of

(26) Warrener, R.; Pitt, I. G.; Butler, D. N. *J. Chem. Soc., Chem. Commun.* **1983**, 1340–1342.
(27) (a) Paddon-Row, M. N.; Cotsaris, E.; Patney, H. K. *Tetrahedron* **1986**, *42*, 1779–1788. (b) Paddon-Row, M. N. *Acc. Chem. Res.* **1982**, *15*, 245–251.
(28) Mitsudo, T.; Kokuryo, K.; Shinsugi, T.; Nakagawa, Y.; Watanabe, Y.; Takegami, Y. *J. Org. Chem.* **1979**, *44*, 4492–4496.
(29) Smith, C. D. *J. Am. Chem. Soc.* **1966**, *88*, 4273–4274.
(30) Kaupp, G.; Prinzbach, H. *Chem. Ber.* **1971**, *104*, 182–204.
(31) Paquette, L. A.; Bellamy, F.; Bohm, M. C.; Gleiter, R. *J. Org. Chem.* **1980**, *45*, 4913–4921.
(32) Weller, A. *Z. Phys. Chem.* **1982**, *133*, 93–98.
(33) Rehm, D.; Weller, A. *Ber. Bunsges. Phys. Chem.* **1969**, *73*, 834–845.
(34) Breslow, R. *Pure Appl. Chem.* **1974**, *40*, 493–509.
(35) Pasman, P.; Rob, F.; Verhoeven, J. W. *J. Am. Chem. Soc.* **1982**, *104*, 5127–5133.

the fluorescence maximum for this donor in a number of solvents are given in Table I.

As expected[35] the acceptor **3** is nonfluorescent, and its absorption spectrum shows a single $\pi \rightarrow \pi^*$ transition at 228 ± 1 nm (15 500 ± 500 M^{-1} cm^{-1}) virtually independent of the solvent employed. The absorption spectrum of the donor **2** is more complex. In all solvents a pronounced shoulder appears at 328 ± 2 nm tentatively assigned to the vibrational zero–zero transition of the $S_0 \rightarrow S_1$ electronic transition, the vibrational progression of which is apparently masked by the stronger $S_0 \rightarrow S_2$ transition but shows up clearly in the fluorescence ($S_1 \rightarrow S_0$) especially in apolar solvents (see Figure 2A). While the absorption of **2** is virtually solvent independent, its emission undergoes a distinct Stokes shift (see Table I) in more polar media. This indicates that the polarity of the first $\pi \rightarrow \pi^*$ excited state of **2** is significantly increased with respect to that of the electronic ground state and is therefore stabilized by solvation via the reorientation polarization of dipolar solvent molecules prior to fluorescence. It was observed that the fluorescence of **2** is quenched by **3** in a diffusion-limited process in polar as well as in apolar media. Since the absorption data exclude energy transfer from **2** to **3**, electron-transfer quenching seems the most plausible mechanism.

From the electrochemical and photophysical data presented above a reasonably good estimate can be made of the Gibbs free-energy change for electron transfer between **2** in its S_1 excited state and **3** in its electronic ground state. For large intermolecular separation and in acetonitrile as a solvent this is simply given by eq 2.[32,33] For the E_{00}(**2**) term we take the energy of the zero–zero transition in the absorption spectrum of **2** (328 nm, corresponding to 3.78 eV). We note that, especially in polar solvents, a slightly lower value might be appropriate in view of the fluorescence Stokes shift of **2** in such solvents (see Table I); however, we make the simpler assumption here, which leads to $\Delta G(\infty) = -0.98 \pm 0.1$ eV in acetonitrile. At finite distances this must be modified to account for the Coulombic attraction energy between the radical ion pair, which is to a first approximation given by a point-charge model as $-e^2/(\epsilon R_c)$, where R_c indicates the center-to-center distance of the ions and ϵ the dielectric constant of the medium. The dielectric constant also influences the solvation free energy of the ions. This effect is included in the electrochemical redox potentials for acetonitrile but should be corrected for if we wish to apply these potentials to calculate ΔG in different solvents.[36a] According to the Born equation, the solvation free energy of an ion pair is given by eq 3, where r_{d^+} and r_{a^-} are effective radii of the cation and the anion radical.

$$\Delta G_{solv} = -(e^2/2)\{(1/r_{d^+}) + (1/r_{a^-})\}(1 - 1/\epsilon) \qquad (3)$$

From eq 2 and 3 and under correction for the Coulombic attraction, eq 4 is derived[32] for calculation of the free-energy change of photoinduced electron transfer between **2** and **3** in a medium with dielectric constant ϵ at a distance R_c, from the electrochemical data obtained in acetonitrile (ϵ = 37). An al-

$$\Delta G = F[E_{ox}(\mathbf{2}) - E_{red}(\mathbf{3})] - E_{00}(\mathbf{2}) - (e^2/\epsilon R_c) - (e^2/2)\{(1/r_{d^+}) + (1/r_{a^-})\}(1/37 - 1/\epsilon) \qquad (4)$$

ternative form of eq 4 is 4a where ΔG_{vac} is the free-energy change in the gas phase, which ranges from +0.08 eV for **1(4)** to +1.17 eV for **1(12)**.

$$\Delta G = \Delta G_{vac} + e^2\{(1/2r_{d^+}) + (1/2r_{a^-}) - (1/R_c)\}(1/\epsilon - 1) \qquad (4a)$$

The effective radii r_{d^+} and r_{a^-} are model-dependent parameters. It has been found[36b] that a reasonable fit to Born charging energies of aromatic ions is obtained when r_{d^+} is obtained from the molar volume of the neutral molecule, according to $4\pi r^3/3 = M/N\rho$, where N is Avogadro's number, M is the molecular weight, and ρ the density of the crystal. For naphthalene, using standard data,

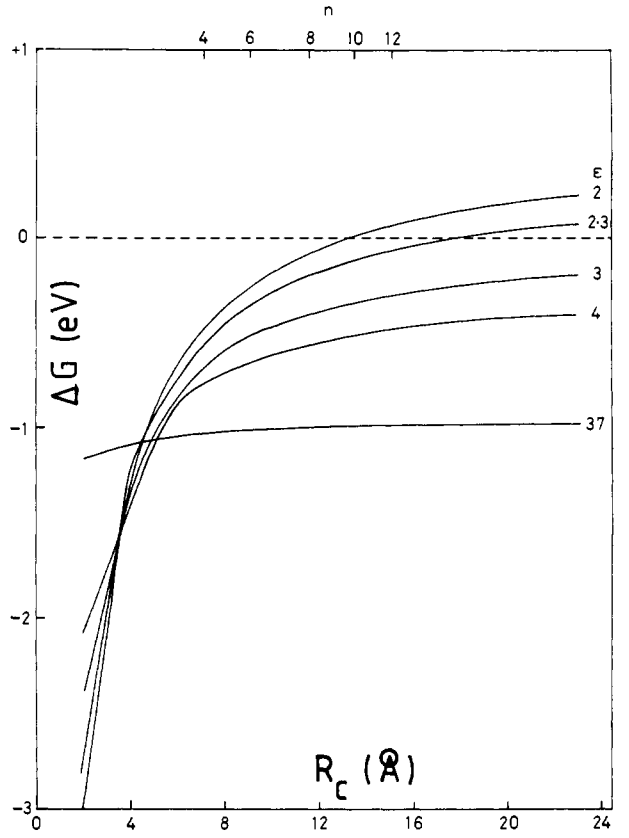

Figure 3. Calculated (via eq 5 with r = 4.5 Å) Gibbs free energy change (ΔG) accompanying photoinduced electron transfer between **2** and **3** as a function of the center-to-center distance (R_c) in solvents of various dielectric constant (ϵ). At the top the R_c values obtained in the molecules **1**(n) have been indicated.

this yields r_{d^+} = 3.7 Å. We would anticipate an effective r_{d^+} for the substituted naphthalene **2** to be larger than this. Under the assumption $r_{d^+} = r_{a^-} = r$ and upon substitution of the appropriate redox and E_{00} values, eq 4 reduces to 5

$$\Delta G = -0.98 - (14.45/\epsilon R_c) - (14.45/r)(1/37 - 1/\epsilon)\ \text{eV} \qquad (5)$$

This implies that in cyclohexane (ϵ = 2.015) and at the formal contact distance ($R_c = 2r$) the driving force is given by $\Delta G = -0.98 + (3.2/r)$. From the diffusion-controlled electron-transfer quenching of **2** by **3** in cyclohexane (vide supra) it may be concluded[33] that even in this apolar medium a driving force of at least 0.2–0.3 eV remains for photoinduced electron transfer in a contact pair of **2** and **3**. From this a value r = 4.1–4.7 Å is suggested for the effective ionic radii. As we shall show later a value $r \approx$ 4.5 Å also is appropriate to describe the solvation of the dipolar excited state resulting from intramolecular electron transfer in **1**. Figure 3 shows how ΔG varies with R_c, as calculated from eq 5 with r = 4.5 Å for solvents of various dielectric constant.

The Influence of the Bridge Length on the Possibility of Photoinduced, Intramolecular Electron Transfer in 1(n). From Figure 3 it appears that in saturated hydrocarbons ($\epsilon \approx 2$) photoinduced electron transfer between **2** and **3** is thermodynamically feasible at short distances only. In fact, the predicted distance at which $\Delta G(R_c)$ becomes zero is 13.3 Å, i.e., just the center-to-center separation in the 10-bond bridged molecule **1(10)**. Even in slightly more polar solvents, however, long-range photoinduced electron transfer could occur if this is fast enough to compete with other relaxation processes. That this requirement can be fulfilled even at a remarkably long distance is demonstrated most dramatically by the behavior of **1(12)**, in which a donor and an acceptor identical with **2** and **3** are rigidly held at a center-to-center distance $R_c \approx$ 15 Å. In saturated hydrocarbon solvents, the fluorescence of **1(12)** is indistiguishable from that of **2** both in lifetime and in quantum yield. As evident from comparison of the data in Table II with those in Table I, however, the fluorescence of **1(12)** is

(36) (a) Electrochemical studies in other solvents, using ultramicroelectrodes are in progress (Lay, P. et al., to be published). (b) Lyons, L. E. *Nature (London)* **1950**, *166*, 193.

Table II. Donor Fluorescence Data for **1(12)** in Various Solvents and Calculated Rates of Photoinduced, Intramolecular Electron Transfer (k_{et})

solvent (ϵ)		λ_{max} (nm)	τ^a (ns)	ϕ^b	k_{et}^c ($s^{-1} \times 10^8$)
cyclohexane	(2.015)	350	5.40	0.35	
benzene	(2.28)	368	1.03	0.10	7.3 (5.3)
di-*n*-butyl ether	(3.10)	354	1.92	0.13	3.1 (1.8)
diethyl ether	(4.20)	357	1.74	0.12	3.7 (2.8)
ethyl acetate	(6.02)	368	1.16	0.17	6.3 (3.0)
tetrahydrofuran	(7.58)	370	0.65	0.06	13.0 (7.8)
acetonitrile	(37.50)	386	2.71	0.18	1.6 (1.8)

[a] Excitation at 303 nm, see Experimental Section. [b] Excitation at 300 nm. [c] Calculated via eq 6 (or via eq 7).

quenched in more polar solvents with a corresponding decrease of its lifetime. Since the measurements were made at a concentration ($\leq 5 \times 10^{-5}$ M) sufficiently low to exclude intermolecular interaction and since the photophysical properties of the donor and acceptor exclude the occurrence of intramolecular energy transfer, we are forced to conclude that intramolecular electron transfer occurs upon excitation of the dimethoxynaphthalene donor in **1(12)** in solvents of intermediate and high polarity.

Under the assumption of irreversibility,[37] the rate constant (k_{et}) of this electron transfer can be calculated either from the lifetimes of **2** and **1(12)** [Tables I and II, respectively] via eq 6 or from their fluorescence quantum yields and the lifetime of **2** via eq 7.

$$k_{et} = 1/\tau(\mathbf{1}) - 1/\tau(\mathbf{2}) \quad (6)$$

$$k_{et} = \{\Phi(\mathbf{2}) - \Phi(\mathbf{1})\}/\{\tau(\mathbf{2})\Phi(\mathbf{1})\} \quad (7)$$

The k_{et} values obtained via eq 6 and 7 are also compiled in Table II. Although the agreement is not perfect (eq 7 systematically giving lower k_{et} values, vide infra), the results convincingly show that photoinduced electron transfer in **1(12)** is fast enough to allow its occurrence in >50% of the molecules primarily excited, in solvents of moderate and high polarity. In a parallel study of the time resolved microwave conductivity of **1(12)** in benzene (ϵ = 2.28) the occurrence of photoinduced charge separation was unequivocally confirmed,[1c] and furthermore the driving force was estimated to be $\Delta G = -0.1$ eV in close accordance with the value of −0.08 eV calculated via eq 5 for photoinduced electron transfer over a distance corresponding to a 12-bond separation (R_c = 14.9 Å).

Having established that photoinduced electron transfer in **1(12)** occurs at >50% efficiency, it comes as no surprise that this process occurs quantitatively or nearly quantitatively[1b] in the shorter homologues leading to an almost complete quenching of the characteristic dimethoxynaphthalene fluorescence. Under these circumstances, application of eq 7 is no longer possible, since the overall fluorescence quantum yield becomes critically dependent upon the presence of minor fluorescent impurities. For **1(8)** and **1(10)**, however, the residual fluorescence of the dimethoxynaphthalene chromophore is still strong enough to be detected by time resolved fluorescence measurements (cf. Experimental Section) as a short-lived component above the longer lived impurity background (see Figure 4). Via a biexponential fitting procedure, the lifetime of this residual fluorescence was determined (cf. Table III) to give k_{et} by application of eq 6.

For **1(4)** and **1(6)** no short-lived fluorescence component could be detected at 360 nm. In view of the available time resolution (cf. Experimental Section) as well as on the basis of other evidence (vide infra) we conclude that $k_{et} \geq 10^{11}$ s^{-1} in **1(4)** and **1(6)**, irrespective of solvent polarity.

As far as we are aware the data compiled in Table III constitute the first direct measurements of the rate of photoinduced electron transfer between a single rigidly oriented donor–acceptor pair at a number of precisely defined distances. We note the remarkably large value of the rate constants for electron transfer via long rigid nonconjugated bridges.

(37) In marginally polar solvents (benzene, di-*n*-butyl ether) indications for partial reversibility have been found; see: ref 1c.

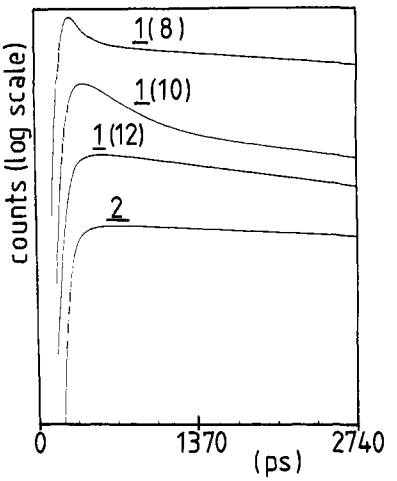

Figure 4. Time-resolved fluorescence measured by single-photon counting (excitation at 303 nm with laser pulses of 7 ps fwhm, see Experimental Section, detection at 360 nm) of **2** and **1(*n*)** (*n* = 8, 10, 12) in di-*n*-butyl ether at 24 °C.

The Influence of Solvent Polarity on Intramolecular Photoinduced Charge Separation Dynamics. The rates k_{et} (cf. Table III) of photoinduced electron transfer in the molecules **1(*n*)** have been studied in solvents which vary widely in dielectric properties. We now turn to consider the theory of such processes. In doing so, we shall not at this stage consider explicitly specific short-range solute–solvent interactions but shall assume, as above, that the solvent is a uniform dielectric characterized by static and optical dielectric constants ϵ and ϵ_o, respectively, at the temperature considered. Furthermore, we shall assume that a high-temperature formalism, in which vibrational tunnelling through the potential barrier is considered negligibly small, is applicable. Thus the rate constant takes the simple form

$$k_{et} = A \exp(-\Delta G^{\ddagger}/k_B T) \quad (8)$$

where $\Delta G^{\ddagger}$ is the free energy of activation, which is a function of both the overall free-energy change (ΔG) and the reorganization energy (λ) accompanying electron transfer.

The reorganization energy can formally be partitioned into an intramolecular part, λ_i, and a contribution from inertial solvent reorganization, λ_s

$$\lambda = \lambda_i + \lambda_s \quad (9)$$

On these assumptions, the free energy of activation is given[38-40] by eq 10

$$\Delta G^{\ddagger} = (\lambda + \Delta G)^2/(4\lambda) \quad (10)$$

This implies that the optimal conditions for electron transfer ($\Delta G^{\ddagger} = 0$) are attained if $-\Delta G = \lambda$.

As discussed above, the solvent has a very large influence on ΔG (see eq 5 and Figure 3), and therefore it might be expected at first sight that the a large solvent effect also applies for $\Delta G^{\ddagger}$. We[25] and others[18] have previously stressed, however, the compensatory roles of solvent-induced changes in ΔG and λ_s in electron-transfer processes between a pair of weakly coupled donor and acceptor species for which electron transfer occurs close to the thermodynamic optimum ($-\Delta G \approx \lambda$). As we shall show later the internal reorganization energy is given by $\lambda_i \approx 0.6$ eV, a value assumed to be solvent independent. The solvent reorganization energy λ_s is given,[39] in a usual approximation, by

$$\lambda_s = e^2(1/r - 1/R_c)(1/\epsilon_o - 1/\epsilon) \quad (11)$$

Substitution of 4a, 9, and 11 into 10 gives eq 12

$$\Delta G^{\ddagger} = \frac{\{\Delta G_{vac} + e^2(1/r - 1/R_c)(1/\epsilon_o - 1) + \lambda_i\}^2}{4e^2(1/r - 1/R_c)(1/\epsilon_o - 1/\epsilon) + 4\lambda_i} \quad (12)$$

(38) Marcus, R. A. *J. Chem. Phys.* **1965**, *43*, 679–701.
(39) Hush, N. S. *Trans. Faraday Soc.* **1961**, *57*, 557–580.

Table III. Donor Fluorescence Lifetime (τ) and Calculated (via eq 6) Rates of Photoinduced, Intramolecular Electron transfer (k_{et}) for **1**(n), n = 8, 10, 12 in Various Solvents at 24 °C

	1(8)		**1(10)**		**1(12)**	
solvent	τ (ps)	k_{et} ($s^{-1} \times 10^8$)	τ (ps)	k_{et} ($s^{-1} \times 10^8$)	τ (ps)	k_{et}($s^{-1} \times 10^8$)
cyclohexane	48	210	5400		5400	
benzene	19	520	135	72	1030	7.3
di-*n*-butyl ether	21[a]	470	270	35	1920	3.1
diethyl ether	21	470	190	51	1740	3.7
ethyl acetate	22	450	115	85	1160	6.3
tetrahydrofuran	15	670	80	120	650	13.0
acetonitrile	33	300	380	24	2710	1.6

[a] Redetermination of this value gave a somewhat shorter lifetime than reported[1a] earlier (67 ps) at lower time resolution.

Table IV. Long Wavelength Charge-Recombination Fluorescence Emission Maxima (nm [eV]) Observed for **1(4)**, **1(6)**, and **1(8)** at 20 °C

	solvent (Δf_1)[a]					
	n-hexane (0.538)	cyclohexane (0.501)	benzene (0.433)	di-*n*-butyl ether (0.134)	diisopropyl ether (−0.019)	diethyl ether (−0.071)
1(4)	475 [2.61]	475 [2.61]	530 [2.34]	560 [2.21]	570 [2.17]	600 [2.01]
1(6)		450 [2.75]				
1(8)		<430[b] >[2.88][b]				

[a] $\Delta f_1 = (2/\epsilon - 1/\epsilon_o)$. [b] Extremely weak tail on residual donor fluorescence. [c] Excitation at 320 nm.

In this expression, we note that dependence on the static dielectric constant (ϵ) enters only through the solvent reorganization energy in the denominator. This dependence, however, can be quite minute especially if the numerator is small compared to $4\lambda_i$(= 2.4 eV). This condition is met in all compounds **1**, where the value of the numerator ranges from 0.01 eV for **1(4)** to 0.42 eV for **1(12)**.

Figure 5 shows the calculated (according to eq 12, with λ_i = 0.6 eV) dependence of $\Delta G^{\ddagger}$ on R_c in five different solvents spanning the polarity range investigated. The results of these calculations (cf. Figure 5) indicate that for **1(4)** photoinduced electron transfer occurs at nearly optimum conditions ($\Delta G^{\ddagger} < 0.01$ eV) in all solvents even though ΔG becomes more negative by ~0.6 eV in going from cyclohexane to acetonitrile at the R_c value involved (cf. Figure 3). Furthermore, the influence of the solvent polarity upon $\Delta G^{\ddagger}$ at larger R_c values corresponding to those in **1(6–12)** is also predicted to be relatively small. If we assume the preexponential factor A in eq 8 to be solvent independent, we thus predict that for each of the systems **1** studied the rate of intramolecular photoinduced electron transfer will be almost solvent independent, unless it becomes thermodynamically unfeasible.

The experimental data (see Table III) fully corroborate this conclusion, which is, of course, of considerable general importance for the interpretation of medium effects in charge-separation dynamics in biological systems as well as model systems.

It should be noted that the continuum model employed here to describe solvent–solute interaction is, of course, too simple to allow quantitative prediction of specific solvent effects. Thus, while the increase of k_{et} in going from the simple dialkyl ethers to the cyclic ether tetrahydrofuran is predicted almost quantitatively (see Figure 5), the relatively high rates in benzene and the relatively low rates in acetonitrile (see Table III) are not accounted for. Clearly a more detailed discussion of these data will require explicit determination of the solvent effect on $\Delta G^{\ddagger}$ and on the preexponential factor A. We are presently engaged in measuring the effect of temperature on k_{et} in order to obtain such data. Despite the crudeness of the model employed to derive the data plotted in Figure 5, it seems safe to conclude that the barrier to photoinduced electron transfer increases with the length of the bridge. This implies that, especially for the longer bridges, it should be possible to enhance the rate of electron transfer even further by making structural modifications in the donor or acceptor that leads to a lowering of this barrier by shifting the point at which $-\Delta G = \lambda$ to higher R_c values. Thus from the calculated (cf. Figure 5) barrier $\Delta G^{\ddagger} \approx 0.1$ eV for **1(12)**, it is predicted that the rate of electron transfer across such a 12-bond bridge might be increased by one

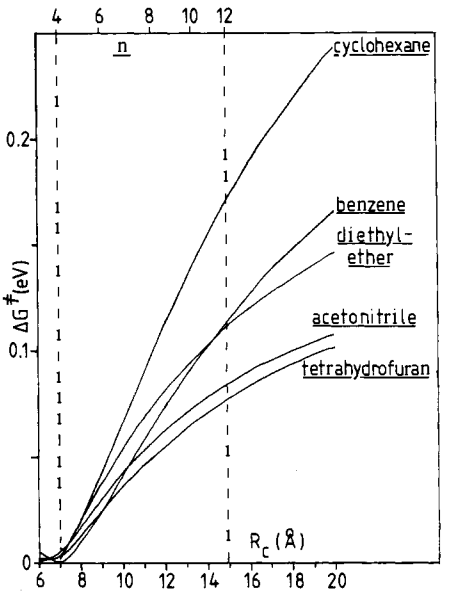

Figure 5. Calculated (via eq 12) with r = 4.5 Å) free energy of activation for photoinduced electron transfer as a function of R_c in various solvents. At the top the R_c values attained in **1(*n*)** have been indicated.

to two orders of magnitude if the redox properties of the donor–acceptor pair are enhanced without changing the preexponential factor. Such structural modifications are being actively pursued.

Charge-Recombination Fluorescence: Estimation of the Mean Ion Radius. While, as remarked earlier, the characteristic emission of the dimethoxynaphthalene system is completely quenched in the molecules **1(4)** and **1(6)**, a new, weak, and broad long-wavelength emission is observed for **1(6)** and especially for **1(4)** in a limited number of solvents with low polarity, while **1(8)** shows a very weak, long-wavelength tail on the residual donor emission. For **1(6)** we were able to detect this emission in cyclohexane (λ_{max} 450 nm), but for **1(4)** it could be studied also in slightly more polar solvents, although its intensity drops steeply as polarity is increased. The broadness and weakness of the emission bands hamper accurate determination of the emission maxima. It is evident, however, that a strong bathochromic shift occurs in more polar solvents (see Table IV), which identifies it as emission arising from an excited state with a highly dipolar character, i.e., the intramolecular charge-separated state.

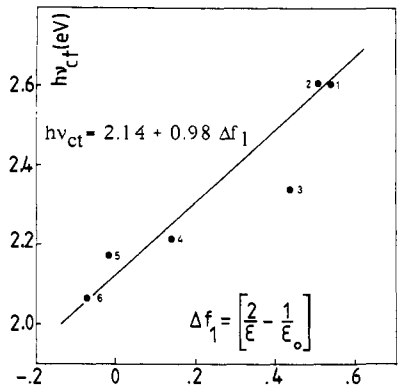

Figure 6. Position of the charges-transfer fluorescence maximum ($h\nu_{ct}$) for **1(4)** as a function of the solvent parameter Δf_1 (see Table IV).

In a related study,[1b,c] the dipole moments of the excited state have been measured for the molecules **1**. These moments are consistent with complete charge transfer in the excited state; that for **1(12)** is 77 Debye,[1c] which is the largest moment so far recorded for a charge-transfer state. The energy, $h\nu_{ct}$, of the vertical transition from the charge-transfer excited state to the ground state ($D^+A^- \rightarrow DA$) can be expressed in terms of overall free energy and reorganization energy accompanying the transition. We write for the reorganization energy λ_{recomb} accompanying the charge recombination

$$\lambda_{recomb} = \lambda_i' + \lambda_s \quad (13)$$

where, by analogy with eq 9, the first and second terms refer to intramolecular and solvent reorganization respectively. In eq 13, it is assumed that the solvent reorganization term is identical with that for the process $D^*A \rightarrow D^+A^-$. Where a continuous dielectric model of the solvent is appropriate, this will be a very good approximation provided that the D^*A state is not significantly more polar than the ground state. There is evidence (vide supra) that this is not exactly so; however, such polarity changes would probably lead to deviations less than the range of uncertainty of the present experimental data. It then follows that the energy of the charge-transfer fluorescence emission maximum is given by

$$h\nu_{ct} = \Delta G + E_{00}(\mathbf{2}) - \lambda_i' - \lambda_s = F\{E_{ox}(\mathbf{2}) - E_{red}(\mathbf{3})\} - e^2/37r - \lambda_i' + e^2(1/r - 1/R_c)(2/\epsilon - 1/\epsilon_o) \quad (14)$$

In Figure 6, the plot of $h\nu_{ct}$ against the solvent factor $\Delta f_1 = (2/\epsilon - 1/\epsilon_o)$ is shown for **1(4)**. Although the number of data points is small, there is evidently a correlation of the kind predicted; the single point that lies off the general trend is that for benzene, which may suggest additional specific stabilization of the charge-separated state by ~0.1–0.2 eV in this solvent.

From the slope (0.98) of the plot in Figure 6 we may obtain an estimate of the average radius r of the donor radical cation and the acceptor radical anion, since we know the center-to-center distance R_c = 7Å. Thus $0.98 = 14.45(1/r - 1/7)$, which gives r = 4.75 Å, a value close to that (~4.5 Å) obtained above from consideration of the electron-transfer quenching dynamics of **2** by **3**.

Equation 14 may also be employed to predict $h\nu_{ct}$ for the higher homologues of **1**. In cyclohexane this gives 2.8 and 3.0 eV for **1(6)** and **1(8)**, respectively, which is consistent with the experimental values (see Table IV) of 2.75 and >2.88 eV, respectively, but evidently a larger set of more precise data is necessary to test this dependence quantitatively.

In analyzing both the charge separation and the charge recombination, we have now used a model suitable for widely separated electron donor–acceptor pairs, specifically for a solvent-separated ion pair. This is in accord with the current approach to such electron transfer systems, which are of the "outer-sphere" type. For close contact ion pairs (and also for exciplexes) an alternative approach to interpretation of the solvent dependence of the charge recombination emission frequency has

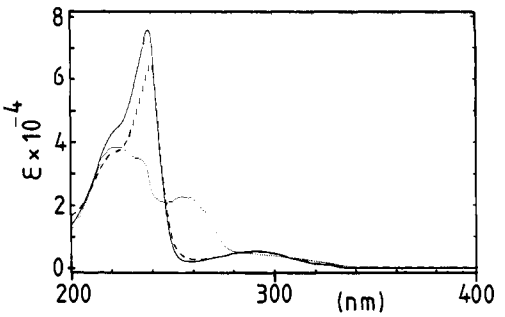

Figure 7. Absorption spectra of **1(4)** (···) and **1(6)** (– – –) as well as the superposition of the spectra of **2** and **3** (—) cyclohexane.

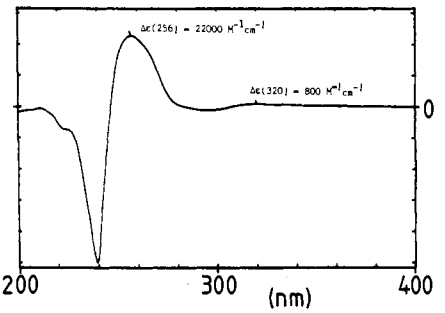

Figure 8. Absorption difference spectrum obtained by subtracting the superposition of spectra of **2** and **3** from that of **1(4)**.

frequently been used:[41,42] in this model, the excited state is represented as a point dipole. We have shown before[1d] that application of this model to **1(4)** leads to an estimate of ~20 Debye for its excited state dipole moment. This has no precise quantitative significance, but it confirms the charge-separated nature of the emissive state. Independent measurement[1b] of the excited state dipole moment by time resolved microwave conductivity gave a value of 24 Debye for **1(4)**.

Absorption Spectroscopic Evidence for Through-Bond Interaction in Nonconjugatively Bridged Molecules 1. Little direct evidence for electronic interaction between donor and acceptor is provided by the electronic absorption spectra of **1(8)**, **1(10)**, and **1(12)**. The situation is quite different, however, for **1(6)** and especially for **1(4)**. While the electronic absorption spectra of the higher homologues are indistinguishable from the superposition of spectra of **2** and **3**, significant broadening is observed for **1(6)**, and for **1(4)** the appearance of two new transitions, not attributable to either individual donor or acceptor, is apparent in a difference spectrum (see Figures 7 and 8).

On the basis of our earlier experience[6,7,35] with the properties of molecules containing bridged donor–acceptor pairs, we attribute these spectral changes to an intramolecular charge-transfer type interaction mediated by electronic interaction via the bridge. The potential of the dimethoxynaphthalene moiety to act as an efficient electron donor in charge-transfer interactions was investigated by studying the formation of intermolecular charge-transfer complexes between **2** and the strong acceptor tetracyanoethylene (TCNE). Figure 9 displays the CT absorption spectrum of **2**/TCNE in the visible region.

Two charge-transfer transitions appear with a separation of 0.73 eV. This compares reasonably well with the separation (0.97 eV) between the two "new" bands observed in **1(4)** by difference spectroscopy (cf. Figure 8) and indicates that in both cases charge-transfer transitions are involved for which in a single particle model the highest occupied molecular orbital Ψ^d_N and the penultimate occupied molecular orbital Ψ^d_{N-1} of the di-

(40) Sutin, N. *Acc. Chem. Res.* **1982**, *15*, 275–282.
(41) Mes, G. F.; de Jong, B.; van Ramesdonk, H. J.; Verhoeven, J. W.; Warman, J. M.; de Haas, M. P.; Horsman-van den Dool, L. E. W. *J. Am. Chem. Soc.* **1984**, *106*, 6524–6528.
(42) Beens, H.; Knibbe, H.; Weller, A. *J. Chem. Phys.* **1967**, *47*, 1183–1184.

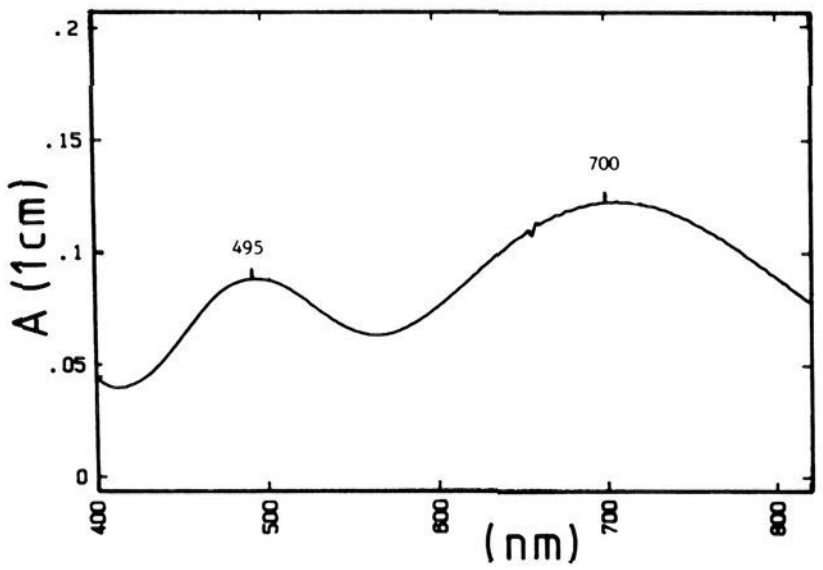

Figure 9. Visible charge-transfer absorption resulting from interaction between **2** (ca. 10^{-4} M) and tetracyanoethylene in dichloromethane at 20 °C.

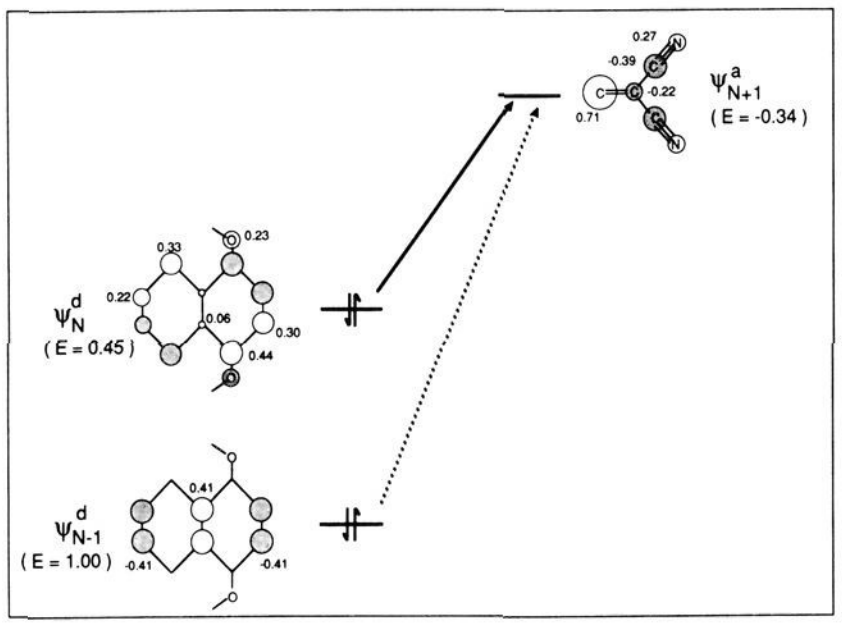

Figure 10. Orbital coefficients and energies (E in β units) for frontier MO's in 1,4-dimethoxynaphthalene and in 1,1-dicyanoethylene as calculated by the Hückel method. The first and second charge-transfer excitation are indicated by drawn and dotted arrows, respectively.

methoxynaphthalene system act as the donor level. A Hückel calculation provides a qualitative interpretation, indicating the presence of two closely spaced occupied levels for this donor (see Figure 10).

According to this simple approach, $\Psi^d{}_N$ and $\Psi^d{}_{N-1}$ are antisymmetric (A″) and symmetric (A′) with respect to the C_s symmetry of **1**. It seems likely that the great difference in intensity of the two charge-transfer bands in **1(4)** (see Figure 8) but not in the intermolecular **2**/TCNE complex (see Figure 9) is related to the symmetry properties of **1**. In **1** the symmetry of the lowest unoccupied acceptor orbital ($\Psi^a{}_{N+1}$ see Figure 10) matches that of $\Psi^d{}_{N-1}$ but not that of $\Psi^d{}_N$.

It is important to stress that the maximum of the lowest energy charge-transfer transition observed in **1(4)** (320 nm = 3.87 eV) coincides very nearly with the E_{00} of the dimethoxynaphthalene unit (3.78 eV). This means that for **1(4)** the potential energy surfaces of the D^+A^- state and the D*A state intersect near the minimum of the latter, thus providing a situation in which no barrier exists for photoinduced intramolecular electron transfer, in accord with what we concluded above (see Figure 5) on the basis of a much more circumstantial thermochemical analysis!

Intramolecular Contribution to Charge-Transfer Reorganization Energy. If the energies of the maxima in charge-transfer absorption and emission are $h\nu_{ct}$(absorption) and $h\nu_{ct}$(emission), we can write on our previous assumptions

$$h\nu_{ct}(\text{absorption}) - h\nu_{ct}(\text{emission}) = 2\lambda' \qquad (15)$$

In the saturated hydrocarbon solvents, where λ_s is zero, the right-hand side of eq 15 reduces to $2\lambda'_i$, i.e., twice the intramolecular reorganization energy accompanying the process DA → D^+A^-. If we furthermore neglect the internal reorganization energy in the process DA → D*A this also equals $2\lambda_i$, i.e., twice *the internal reorganization energy for the photoinduced charge* separation process D*A → D^+A^-.

For **1(4)** the experimental parameters entering eq 15 are available. Thus from the difference spectrum in Figure 8 $h\nu_{ct}$(absorption) = 3.87 eV is estimated, a value not expected to depend significantly on the medium (vide infra), while $h\nu_{ct}$(emission) = 2.61 eV in saturated hydrocarbon solvents (see Table V) whence $\lambda_i \simeq 0.5(3.87 - 2.61) \approx 0.6$ eV. It is reasonable to expect that this value will not depend significantly on the length of the bridge since most of the internal reorganization is confined to the donor and acceptor moieties.

Alternatively a value for λ_i may be derived from $h\nu_{ct}$(absorption) alone, since (under the assumptions made above and with the use of eq 4 and 11 this is given by

$$h\nu_{ct}(\text{absorption}) = \Delta G + \lambda_i + \lambda_s + E_{00}(\mathbf{2}) = F\{E_{ox}(\mathbf{2}) - E_{red}(\mathbf{3})\} - e^2/37r + \lambda_i + (e^2/\epsilon_o)(1/r - 1/R_c) \qquad (16)$$

Equation 16 confirms that the charge-transfer absorption maximum must be nearly solvent independent, since in contrast to the position of the emission maximum (see eq 14) it is predicted to be a function of the optical dielectric constant only. Upon substitution of the appropriate parameters eq 16 gives $h\nu_{ct}$(absorption) = 3.28 + λ_i (in eV) for **1(4)** in solvents with $\epsilon_o = 2$. The experimental value of 3.87 eV thus leads to $\lambda_i \approx 0.6$ eV, which is consistent with the value derived above and furthermore also compares well with the λ_i value found for electron transfer in the radical anion of **1** during a parallel study employing pulse radiolysis techniques.[43]

Distance Dependence of Photoassisted Electron-Transfer Rates. A major aim of the project of which this work is a part is to obtain experimental insight into the manner in which the rate of photoassisted electron transfer is modulated by the bridge linking the donor and acceptor groups. We have used in the work reported here only one type of bridge, the length of which was increased incrementally, so that modulation of the transfer rate by the length of this particular bridge is the point on which we focus. In later extensions it is planned to use bridges modified so as to systematically vary the extent of $\sigma-\pi$ coupling at a given length. Until quite recently, there has been a very general tendency to regard nonconjugated bridges, both in naturally occurring biological and in model systems, as fulfilling a purely geometrical role, hence the common term "spacer" for such bridges. However, the possibility of very appreciable $\sigma-\pi$ interaction through such linkages, leading to significant mediated electronic coupling of donor and acceptor, has recently come to be recognized.[6,22,24,35,44-48] A consequence not without irony of the efficiency as $\sigma-\pi$ coupling mediators of the bridges employed in the present study is that at distances up to and including 6-bond separation the photoinduced electron transfer time is less than the resolution of ~10 ps of our measurements. Consequently, as far as quantitative data are concerned, we are limited to rates for the three molecules with 8-, 10-, and 12-bond separation. Thus at this point only some very general conclusions can be drawn. The rate constant for electron transfer (see eq 8) can be written in more detail as

$$k_{et} = \kappa A_0 \exp(-\Delta G^{\ddagger}/k_B T) = k_{et}(\text{optimal}) \exp(-\Delta G^{\ddagger}/k_B T) \qquad (17)$$

In (17) the preexponential term is now factored into the product of an electronic transmission coefficient κ and A_0 (A_0 is of the order 10^{12}–10^{14} s^{-1} and is a function, inter alia, of the vibration

(43) Miller, J. R. et al., to be published.
(44) Stein, C. A.; Lewis, N. A.; Seitz, G. *J. Am. Chem. Soc.* **1982**, *104*, 2596–2599.
(45) Hush, N. S. *Coord. Chem. Rev.* **1985**, *64*, 135–157.
(46) Beratan, D. N.; Hopfield, J. J. *J. Am. Chem. Soc.* **1984**, *106*, 1584–1594.
(47) Beratan, D. N. *J. Am. Chem. Soc.* **1986**, *108*, 4321–4326.
(48) Larsson, S.; Matos, J. M. O. *J. Mol. Struct.* **1985**, *120*, 35–40.

Table V. Calculated Barriers to Electron Transfer and Optimal Rates of Electron Transfer in Various Solvents as Calculated According to eq 17[a]

	1(8)		1(10)		1(12)	
solvent	$\Delta G^{\ddagger}$ (eV)	k_{et}(opt) ($s^{-1} \times 10^{11}$)	$\Delta G^{\ddagger}$ (eV)	k_{et}(opt) ($s^{-1} \times 10^{11}$)	$\Delta G^{\ddagger}$ (eV)	k_{et}(opt) ($s^{-1} \times 10^{-11}$)
cyclohexane	0.10	10.64				
di-*n*-butyl ether	0.074	8.58	0.096	1.52	0.111	0.242
diethyl ether	0.074	8.58	0.096	2.21	0.111	0.288
tetrahydrofuran	0.049	4.60	0.065	1.54	0.077	0.267

[a] Via eq 12, see also Figure 5.

frequencies involved in coupling vibrational and electronic motion).

For the photoinduced electron transfer in **1** the distance dependence of k_{et} is contained both in $\Delta G^{\ddagger}$ and in κ. The distance and solvent dependence of $\Delta G^{\ddagger}$ was discussed above in the framework of a simple continuum model (see Figure 5 and eq 12). As we have stressed, this treatment is unable to account for eventual specific solvent effects. The behavior, however, of the charge-transfer fluorescence emission as a function of solvent (see Figure 6) suggests that a continuum model is quite adequate to describe the solvation by saturated hydrocarbons and by monoether solvents. In four such solvents (i.e., cyclohexane, di-*n*-butyl ether, diethyl ether, and tetrahydrofuran) k_{et} values are available (see Table III) although in cyclohexane this is limited to that for **1(8)**. Table V compiles the $\Delta G^{\ddagger}$ values as calculated via eq 12 for **1(8)**, **1(10)**, and **1(12)** in these solvents together with k_{et}(optimal) as obtained upon substitution of $\Delta G^{\ddagger}$ in eq 17 together with the experimental k_{et} data from Table III.

As stated, an important aim of this research is to establish the actual functional form of the distance dependence of k_{et}(optimal). Since the data in Table V refer to only three different distances this goal is, as yet, not within reach. Nevertheless it seems interesting to compare the distance dependence of k_{et}(optimal) inferred above with data published by other investigators studying different inter- and intramolecular electron-transfer processes. For purposes of comparison (without the implication that this will represent the variation well at larger or smaller distances), we use her a single exponential fit to the k_{et}(optimal)/distance dependence, since this has been most commonly assumed in related work. As shown in Figure 11 the data from Table V can be fitted rather well by an exponential distance dependence according to eq 18, where R_e gives the edge-to-edge donor–acceptor distance (see Figure 1) which is related to the number of bonds separating donor and acceptor by the relation $R_e = 1.15n$

$$k_{et}(\text{optimal}) = 2.5 \times 10^{15} \exp(-0.85R_e) = 2.5 \times 10^{15} \exp(-0.98n) \quad (18)$$

Although it should be stressed once more that the eq 18 is not intended as a general distance dependence law for through-bond mediated electron transfer, it is interesting to compare it to eq 19 proposed by Miller et al.[2] for intermolecular electron transfer in an MTHF glass again by using a single exponential

$$k_{et}(\text{optimal, intermolecular}) = 10^{13.9} \exp(-1.20R_e) \quad (19)$$

The problems[22] inherent in defining R_e in an intramolecular situation make comparison of the preexponential factors in (18) and (19) less meaningful. Qualitatively, however, (18) predicts a much smaller decrease of k_{et} as the distance increases.

Thus, as expected, eq 18 predicts that especially at larger distances intramolecular electron transfer mediated by through-bond interaction will be much more efficient than intermolecular electron transfer. The efficiency of the present bridges to mediate electron transfer emerges even more clearly if we compare eq 18 with a recent estimate[15] for intermolecular electron transfer occurring under optimally exothermic conditions in a complex of two redox proteins with a known $R_e = 8.5$ Å between the redox centers. At this separation eq 18 predicts $k_{et} = 1.8 \times 10^{12}$ s^{-1} while a rate constant of only 5×10^5 s^{-1} was reported, thus demonstrating the dramatic enhancement that efficient through-bond interaction can exert on the rate of long-range electron transfer!

It can be shown[38-40] that for weak coupling ($J \leq k_BT$) the electronic transmission coefficient should become proportional to the square of the electronic coupling energy (J) between donor and acceptor. We do not so far have a direct measurement of J for the photoinduced electron transfers. From the photoelectron spectra, however, of dienes linked by the same type of bridges with $n = 3$, 4, 5, and 6, a splitting (ΔIP) of the π-ionization potential has been observed[27] which is related to the electronic through-bond interaction energy in such dienes, assuming $\Delta IP \approx 2J$. Over the range studied, ΔIP can be fitted to the expression (20)

$$\Delta IP = \exp(1.56 - 0.46n) \quad \text{in eV} \quad (20)$$

Extrapolation of these results leads to a value of $[J(n = 8)/J(n = 12)]^2 \approx 40$. This if fortuitously close to the ratio of k_{et}(optimal) for **1(8)** and **1(12)** derived from eq 18, which is $7.72/0.24 = 32$. However, on the reasonable assumption that variation of J with n will be similar in molecules **1(*n*)** and the dienes, this comparison lends strong support to identification of the donor–acceptor coupling mechanism responsible for the remarkably fast electron transfer in **1(*n*)** as through-bond interaction. It also corroborates the predictions made from both theoretical[49] as well as earlier experimental studies employing photoelectron and electron-transmission spectroscopy[27,50-53] that this through-bond interaction falls off rather slowly with distance. In this respect the bridges incorporated in the present systems seem to be remarkably effective

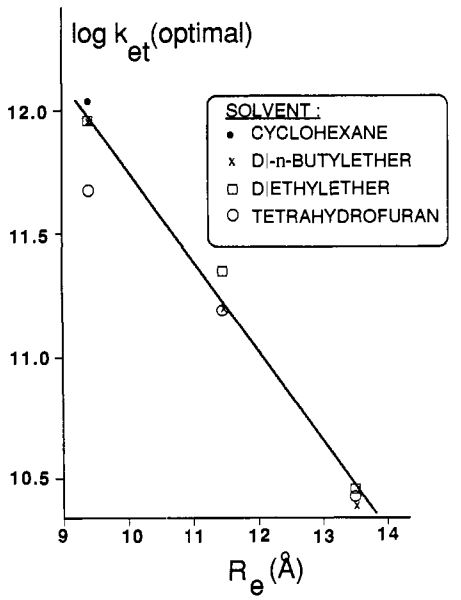

Figure 11. Estimated (see Table V) optimal rates of photoinduced electron transfer across, the bridges of **1(8)**, **1(10)**, and **1(12)** as a function of the donor–acceptor edge-to-edge distance (R_e) in various solvents.

(49) Hoffmann, R.; Imamura, A.; Hehre, W. J. *J. Am. Chem. Soc.* **1968**, *90*, 1499–1509.
(50) Paddon-Row, M. N.; Patney, H. K.; Peel, J. B.; Willett, G. D. *J. Chem. Soc. Chem. Commun.* **1984**, 564–566.
(51) Paddon-Row, M. N.; Patney, H. K.; Brown, R. S.; Houk, K. N. *J. Am. Chem. Soc.* **1981**, *103*, 5575–5577.
(52) Jorgensen, F. S.; Paddon-Row, M. N.; Patney, H. K. *J. Chem. Soc., Chem. Commun.* **1983**, 573–575.
(53) Jorgensen, F. S.; Paddon-Row, M. N. *Tetrahedron Lett.* **1983**, *24*, 5415–5418.

since in recent studies employing different types of nonconjugating bridges a significantly faster decrease of the through-bond coupling with increasing number of σ-bonds was observed[22,24] or predicted.[47]

While the exponential part in (18) is thus probably typical of the type of bridges used here, the preexponential factor is expected to depend not only on the nature of the bridge but also on the electronic structure of donor and acceptor, more in particular on the energy, spatial distribution, and symmetry of the frontier orbitals involved.

Concluding Remarks. The data presented above provide unambiguous evidence for the important influence of the intervening medium on the rate of electron transfer. Furthermore, it has been shown that the thermodynamic and optical data can be correlated in a simple theoretical framework. In particular, the at first sight very surprising near-independence of photoinduced charge separation rates on solvent type for reactions calculated to differ by as much as ~0.9 eV in driving force has a ready interpretation in terms of simultaneous accompanying variation in solvent reorganization energy. The results are general and will be of particular significance for biological photoinduced electron transfers.

One of the most remarkable features of our results (anticipated from theoretical and experimental studies on the bridges used) is the observation that a saturated hydrocarbon bridge can be highly effective in mediating electron transport. This is evident not only from comparison of our data with those obtained for intermolecular electron transfer but also from comparison with experiments where redox centers are linked by other types of bridges including polypeptides[10-16] and partly unsaturated bridges.[24] In this connection it seems important to draw attention to earlier reports of Kuhn et al.[4,5] who obtained evidence for electron transfer (attributed to tunneling) on a ns time scale across monolayers (20–30-Å thickness) of fatty acid molecules in Langmuir–Blodgett film assemblies. In these monolayers, the paraffinic polymethylene chains adopt a stretched conformation similar to that present in the backbone of the rigid bridges in molecules **1**. It has been shown by theory[49] as well as by experiment[27] that such a conformation optimizes the through-bond interaction which we believe is responsible for the remarkably fast long-range electron transfer in **1**.

Much more information and more detailed theory will be needed to understand in detail the effect of the molecular and spatial structure of the "intervening medium" on electron transfer. Such information is essential to reveal the factors governing electron transport in many biological redox processes, as well as for the design of artificial systems aiming at energy conversion or information processing via electron transfer at the molecular level. Rigid systems related to those studied here appear to be of great value in such studies as well as in those directed toward quantitative understanding of the energetics and dynamics of solvation of dipolar species.

Experimental Section

Syntheses. Dicyanomethylene Compound 1(8). The synthesis of this compound has been reported previously.[27]

(1α,4α,4aα,5β,12β,12aα)-1,2,3,4,4a,5,12,12a-Octahydro-1,4:5,12-dimethano-6,11-dimethoxynaphthacene (2). A magnetically stirred solution of **4**[27a] (200 mg, 0.63 mmol) in EtOAc (25 mL), containing 10% Pd/C (100 mg), was hydrogenated at 1 atm and 25 °C until uptake of hydrogen had ceased. The mixture was filtered, and the filtrate was evaporated to give **2** in quantitative yield. Recrystallization from acetone gave a pure sample, mp 139–140 °C: ^{1}H NMR (300 MHz, $CDCl_3$) δ 1.37–1.70 (br m, 7 H), 2.01 (s, 2 H), 2.18 (d, J = 10.4 Hz, 1 H), 2.41 (br s, 2 H), 3.58 (br s, 2 H), 3.98 (s, 6 H, 2 × OCH_3), 7.41–7.44 (m, 2 H), 8.03–8.07 (m, 2 H). Anal. Calcd for $C_{22}H_{24}O_2$: C, 82.46; H, 7.45. Found: C, 82.86; H, 7.41.

(1α,4α,4aα,5β,8β,8aβ)-1,2,3,4,4a,5,6,7,8,8a-Decahydro-1,4:5,8-dimethanonaphthalen-10-one (5c) and the 10-Dicyanomethylene Derivative 3. A solution of **5a**[54] (6.5 g, 29.6 mmol) in EtOAc (50 mL) containing 10% Pd/C (200 mg) was hydrogenated (1 atm, 25 °C). Workup of the mixture gave **5b** (6.3 g, 96%). This material was immediately subjected to deacetalization. A solution of **5b** (6.3 g) in a mixture of THF (50 mL) and 40% aqueous H_2SO_4 (40 mL) was stirred at 25 °C for 24 h, after which time it was neutralized with aqueous $NaHCO_3$ and then extracted with CH_2Cl_2. The dried (Na_2SO_4) CH_2Cl_2 extract was evaporated at 1 atm, and the residue was distilled (110 °C/113 mm) to give the ketone **5c** (2.4 g, 46%) as a low melting solid, mp 25–26° C: IR (CCl_4, cm^{-1}) 1765 (C=O); ^{1}H NMR (250 MHz, $CDCl_3$) δ 1.1–1.22 (m, 3 H), 1.52–1.59 (m, 2 H), 1.62–1.71 (m, 2 H), 1.84–1.93 (m, 6 H), 1.99 (dt, J = 3.1, 11.3 Hz, 1 H), 2.29 (m, 2 H). Anal. Calcd for $C_{12}H_{16}O$: C, 81.77; H, 9.15. Found: C, 81.82; H, 9.02.

A solution of **5c** (1.0 g, 5.7 mmol), malononitrile (1.1 g, 17.1 mmol), AcOH (1 mL), and NH_4OAc (440 mg) in toluene (50 mL) was refluxed in a Dean–Stark apparatus for 20 h. The cooled mixture was successively washed with saturated aqueous $NaHCO_3$ (100 mL) and water (100 mL). The dried solution was evaporated under reduced pressure, and the resulting residue was passed down a short alumina column (EtOAc). Recrystallization of the eluted material gave **3** (0.75 g, 59%), mp 110–111 °C: IR (CCl_4, cm^{-1}) 2230 (CN), 1645 (C=C); ^{1}H NMR (60 MHz, $CDCl_3$) δ 1.17–2.10 (m, 12 H), 2.37 (br s, 2 H) < 3.00 (br s, 2 H). Anal. Calcd for $C_{15}H_{16}N_2$: C, 80.32; H, 7.19; N, 12.49. Found: C, 80.24; H, 7.22; N, 12.62.

(1α,4α,4aα,5β,12β,12aα)-1,2,3,4,4a,5,12,12a-Octahydro-1,4:5,12-dimethano-6,11-dimethoxynaphthacene-14-one (10(0,0)) and the 14-Dicyanomethylene Derivative 1(4). A mixture of **6(0,0)**[31] (10.0 g, 39.7 mmol) and **12** (10.5 g, 39.8 mmol) was heated at 110 °C for 48 h. Trituration of the reaction mixture with hexane gave a solid which was recrystallized from EtOH to give **9a(0,0)** (16.2 g, 79%), mp 190–191 °C: ^{1}H NMR (60 MHz, $CDCl_3$) δ 1.57 (d, J = 11.0 Hz, 1 H), 1.97 (d, J = 11.0 Hz, 1 H), 2.80 (s, 2 H), 3.48 (s, 3 H, OCH_3), 3.55 (s, 3 H, OCH_3), 3.81 (m, 2 H), 4.02 (s, 6 H, 2 × OCH_3), 7.40–7.63 (m, 2 H), 8.05–8.23 (m, 2 H).

To a refluxing solution of **9a(0,0)** (15.0 g, 29.1 mmol) in THF (100 mL) and absolute EtOH (150 mL) was added small pieces of sodium (40.0 g, 1.7 mol) over a period of 2 h. The mixture was then refluxed for a further 5 h. EtOH (20 mL) was added to the cooled mixture followed by crushed ice (300 g). Extraction with hexane (3 × 150 mL) and evaporation of the organic extracts (after washing with H_2O and drying) gave a thick yellow oil (10.6 g) whose ^{1}H NMR spectrum revealed the presence of **9b(0,0)**, together with compounds resulting from the reduction of the naphthalene ring. Rearomatization was achieved by treating this oil with DDQ (8.23 g, 36.3 mmol) in refluxing benzene (120 mL) for 1 h. The cooled mixture was filtered, and the filtrate washed with aqueous NaOH (170 mL, 0.3 M). Evaporation of the dried filtrate gave a brown oil (10.0 g) which was subjected to column chromatography (alumina; EtOAc/hexane, 25:100). Although the eluted solid (6.9 g) resisted further purification, its ^{1}H NMR spectrum revealed that it consisted of ca. 95% **9b(0,0)**: ^{1}H NMR (60 MHz, $CDCl_3$) δ 1.28 (d, J = 10.4 Hz, 1 H), 2.47 (br s, 2 H), 2.90–3.27 (m, 9 H), 3.61 (br s, 2 H), 3.97 (s, 6 H, 2 × OCH_3), 6.18 (t, J = 2.2 Hz, 2 H), 7.33–7.53 (m, 2 H), 8.00–8.23 (m, 2 H).

Hydrogenation of crude **9b(0,0)** (3.5 g) using identical conditions that were described above for the synthesis of **2** gave, after workup, a light yellow solid (3.4 g), whose ^{1}H NMR spectrum revealed the complete absence of double bond. A solution of this hydrogenated material (3.4 g, 8.9 mmol) in THF (40 mL) and 40% aqueous H_2SO_4 (40 mL) was stirred at 25 °C for 18 h. The usual workup procedure, as described above for the preparation of **5c**, gave the ketone **10(0,0)** (2.5 g, 84%), mp 179–181 °C (from CH_2Cl_2/hexane): IR (CCl_4, cm^{-1}) 1762 (C=O); ^{1}H NMR (60 MHz, $CDCl_3$) δ 1.63–2.47 (m, 10 H), 3.83 (m, 2 H), 3.97 (s, 6 H, 2 × OCH_3), 7.30–7.53 (m, 2 H), 7.90–8.12 (m, 2 H). Anal. Calcd for $C_{22}H_{22}O_3$: C, 79.02; H, 6.63. Found: C, 78.91; H, 6.71.

A solution of **10(0,0)** (1.0 g, 3.0 mmol), malononitrile (594 mg, 9.0 mmol), AcOH (0.6 mL), and NH_4OAc (230 mg) in toluene (15 mL) was refluxed in a Dean–Stark apparatus for 18 h. Usual workup procedure, as described above for the synthesis of **3**, gave an oil which was recrystallized from EtOH to yield **1(4)**, mp 106–107 °C: IR (CCl_4, cm^{-1}) 2241 (CN); ^{1}H NMR (60 MHz, $CDCl_3$) δ 1.70–2.40 (m, 8 H), 3.22 (br s, 2 H), 3.82 (br s, 2 H), 3.96 (s, 6 H, 2 × OCH_3), 7.30–7.50 (m, 2 H), 7.87–8.07 (m, 2 H). Anal. Calcd for $C_{25}H_{22}N_2O_2$: C, 78.51; H, 5.80; N, 7.52. Found: C, 78.64; H, 5.89; N, 7.25.

(1α,4α,4aα,5β,5aα,6β,13β,13aα,14β,14aα)-1,2,3,4,4a,5,5a,6,13,13a,14,14a-Dodecahydro-1,4:5,14:6,13-trimethano-7,12-dimethoxypentacen-15-one (10(1,0)) and Its 15-Dicyanomethylene Derivative (1(6)). A mixture of **6(1,0)**[27a] (3.0 g, 9.43 mmol) and **12** (2.76 g, 10.5 mmol) was heated for 96 h at 110 °C. Addition of hexane (50 mL) to the reaction mixture produced a solid which was recrystallized from MeOH/acetone to give **9a(1,0)** (4.4 g, 80%), mp 262–263 °C: ^{1}H NMR (60 MHz, $CDCl_3$) δ 1.13–2.00 (br m, 6 H), 2.35 (s, 2 H), 2.57 (br s, 2 H), 3.45 (br s, 6 H), 3.72 (br s, 2 H), 4.00 (s, 6 H, 2 × OCH_3), 7.33–7.53 (m, 2 H), 7.93–8.13 (m, 2 H).

(54) McCulloch, R. K.; Rye, A. R.; Wege, D. *Aust. J. Chem.* **1974**, *27*, 1929–1941.

To a stirred solution of **9a(1,0)** (4.0 g, 6.87 mmol) in a refluxing mixture of liquid ammonia (50 mL), THF (80 mL), and *t*-BuOH (4.0 g) were added small pieces of sodium (1.42 g, 61.8 mmol). When the blue color of the mixture was discharged, ice-cold water (200 mL) was added, and the resulting solution was extracted with pentane (3 × 100 mL), dried (Na_2SO_4), and evaporated to give a gummy solid comprising of a mixture of products resulting from partial reduction of the aromatic ring. Treatment of this solid (2.92 g, 6.6 mmol) with DDQ (3.01 g, 13.3 mmol) in dioxan (50 mL) for 17 h at 25 °C gave, after filtration, evaporation of the filtrate and column chromatography (alumina; EtOAc/hexane, 25:100), a solid which was recrystallized from EtOH to give **9b(1,0)** (0.65 g), mp 172–173 °C: ^{1}H NMR (60 MHz, $CDCl_3$) δ 1.43–3.30 (overlapping multiplets, 12 H), 3.00 (s, 3 H, OCH_3), 3.10 (s, 3 H, OCH_3), 3.63 (br s, 2 H), 3.99 (s, 6 H, 2 × OCH_3), 6.05 (t, J = 2.1 Hz, 2 H), 7.30–7.51 (m, 2 H), 7.92–8.12 (m, 2 H).

Catalytic hydrogenation of **9b(1,0)** (0.62 g, 1.4 mmol) using the same conditions as were described for the synthesis of **2**, gave material (0.6 g) whose ^{1}H NMR spectrum revealed the complete absence of double bond. A solution of this hydrogenated material (0.6 g, 1.3 mmol) in a mixture of THF (20 mL) and 40% aqueous H_2SO_4 (20 mL) was stirred at 25 °C for 48 h. The standard workup procedure, as described above for the synthesis of **10(0,0)**, gave, after TLC (EtOAc/hexane, 25:100), the ketone **10(1,0)**, mp 159–160 °C (from EtOH/hexane): IR (CCl_4, cm^{-1}) 1760, 1780 (C=O); ^{1}H NMR (60 MHz, $CDCl_3$) δ 1.57–2.00 (overlapping multiplets, 13 H), 2.46 (d, J = 11.1 Hz, 1 H), 2.53 (br s, 2 H), 3.72 (br s, 2 H), 3.97 (s, 6 H, 2 × OCH_3), 7.30–7.52 (m, 2 H), 7.90–8.12 (m, 2 H). Anal. Calcd for $C_{27}H_{28}O_3$: C, 80.97; H, 7.05. Found: C, 81.20; H, 7.11.

Conversion of **10(1,0)** to the dicyanomethylene derivative **1(6)** was achieved in 73% yield by using the same procedure as described above for the preparation and isolation of **1(4)**. Recrystallization from EtOH gave **1(6)**, mp 241–243 °C: IR (CCl_4, cm^{-1}) 2250 (CN); ^{1}H NMR (60 MHz, $CDCl_3$) δ 1.45–2.30 (overlapping multiplets, 11 H), 2.45 (d, J = 11.2 Hz, 1 H), 2.55 (s, 2 H), 3.02 (br s, 2 H), 3.68 (s, 2 H), 3.97 (s, 6 H, 2 × OCH_3), 7.22–7.44 (m, 2 H), 7.88–8.10 (m, 2 H). Anal. Calcd for $C_{30}H_{28}N_2O_2$: C, 80.33; H, 6.29; N, 6.25. Found: C, 80.01; H, 6.32; N, 6.11.

(1α,4α,4aα,5β,5aα,5bβ,5cα,6β,6aα,7β,14β,14aα,15β,15aα,15bβ,15cα,16β,16aα)-1,2,3,4,4a,5,5a,5c,6,6a,7,14,14a,15,15a,15c,16,16a-Octadecahydro-17-(dicyanomethylene)-1,4:5,16:6,15:7,14-tetramethano-8,13-dimethoxy-5b,15b-dimethylnaphtho[2″,3″:3′,4′]cyclobuta[1′,2′:3,4]cyclobuta[1,2-*b*]naphthacene (1(10)). This compound was prepared from the ketone **10(1,1)**[27a] by using the same procedure as described above for the synthesis and isolation of **1(4)**. Recrystallization from EtOH/EtOAc gave **1(10)** (65%), mp 235 °C dec. IR (CCL_4, cm^{-1}) 2249 (CN); ^{1}H NMR (300 MHz, $CDCl_3$) δ 0.77 (s, 6 H, 2 × CH_3), 1.42 (m, 2 H), 1.54 (d, J = 11.5 Hz, 1 H), 1.57 (s, 2 H), 1.59 (s, 2 H), 1.65 (d, J = 10.6 Hz, 1 H), 1.73 (t, J = 2.5 Hz, 2 H), 1.84 (s, 2 H), 1.85 (s, 2 H), 1.99–2.10 (m, 3 H), 2.22 (s, 2 H), 2.28 (s, 2 H), 2.44 (d, J = 10.5 Hz, 1 H), 2.96 (q, J = 2.3 Hz, 2 H), 3.66 (s, 2 H), 3.98 (s, 6 H, 2 × OCH_3), 7.41–7.44 (m, 2 H), 8.00–8.07 (m, 2 H). Anal. Calcd for $C_{41}H_{42}N_2O_2$: C, 82.79; H, 7.12; N, 4.71. Found: C, 82.38; H, 7.04; N, 4.63.

Dimethyl (2aα,3β,3aα,3bβ,3cα,4β,11β,11aα,11bβ,11cα,12β,12aα)-2a,3,3a,3c,4,11,11a,11c,12,12a-Decahydro-3,12:4,11-dimethano-5,10-dimethoxy-3b,11b-dimethylcyclobuta[1‴,2‴:4″,5″]benzo[1″,2″:3′,4′]cyclobuta[1′,2′:3,4]cyclobuta[1,2-*b*]anthracene-1,2-dicarboxylate (7(0,1)). A magnetically stirred solution of **6(0,1)**[27a] (20.0 g, 50 mmol), DMAD (7.1 g, 50 mmol), and $RuH_2CO(PPh_3)_3$[55] (1.5 g, 1.6 mmol) in benzene (80 mL) was refluxed in a nitrogen atmosphere for 48 h. Ethanol (250 mL) was added to the cooled reaction mixture. The resulting precipitate was recrystallized from EtOH to give **7(0,1)** (25.7 g, 95%), mp 144–146 °C: IR (Nujol, cm^{-1}) 1732; ^{1}H NMR (300 MHz, $CDCl_3$) δ 0.96 (s, 6 H, 2 × CH_3), 1.34 (d, J = 11.5 Hz, 1 H), 1.50 (d, J = 11.4 Hz, 1 H), 1.69 (d, J = 9.8 Hz, 1 H), 1.93 (d, J = 9.8 Hz, 1 H), 1.95 (s, 2 H), 2.19 (s, 2 H), 2.25 (s, 2 H), 2.57 (s, 2 H), 3.66 (s, 2 H), 3.78 (s, 6 H, 2 × OCH_3), 3.98 (s, 6 H, 2 × OCH_3), 7.42–7.45 (m, 2 H), 8.06–8.09 (m, 2 H). Anal. Calcd for $C_{34}H_{36}O_6$: C, 75.53; H, 6.71. Found: C, 75.39; H, 6.82.

Dimethyl (1α,4α,4aβ,4bα,4cβ,5α,5aβ,5bα,5cβ,6α,13α,13aβ,13bα,13cβ,14α,14aβ,14bα,14cβ)-1,4,4a,4c,5,5a,5c,6,13,13a,13c,14,14a,14c-Tetradecahydro-1,4:5,14:6,13-trimethano-7,12-dimethoxy-5b,13b-dimethylbenzo[1⁗,2⁗:3‴,4⁗]cyclobuta[1‴,2‴:3‴,4⁗]cyclobuta[1‴,2‴:4″,5″]benzo[1″,2″:3′,4′]cyclobuta[1′,2′:3,4]cyclobuta[1,2-*b*]anthracene-4b,14b-dicarboxylate (8a(0,1)). A magnetically stirred solution of **7(0,1)** (25.0 g, 46.3 mmol) in quadricyclane (10.0 g, 0.11 mol) was refluxed for 3 days. Acetone (150 mL) was added to the cooled solution, and the resulting precipitate was recrystallized from acetone to give **8a(0,1)** (25 g, 85%), mp 240–241 °C: ^{1}H NMR (300 MHz, $CDCl_3$) δ 0.92 (s, 6 H, 2 × CH_3), 1.08 (d, J = 10.5 Hz, 1 H), 1.60 (d, J = 11.3 Hz, 1 H), 1.67 (d, J = 10.5 Hz, 1 H), 1.81 (d, J = 10.3 Hz, 1 H), 1.90 (d, J = 10.3 Hz, 1 H), 1.91 (s, 2 H), 2.09 (s, 2 H), 2.13 (s, 2 H), 2.16 (s, 2 H), 2.21 (d, J = 11.3 Hz, 1 H), 2.22 (s, 2 H), 2.79 (m, 2 H), 3.62 (s, 2 H), 3.74 (s, 6 H, 2 × OCH_3), 3.96 (s, 6 H, 2 × OCH_3), 6.03 (t, J = 1.8 Hz, 2 H), 7.41–7.45 (m, 2 H), 8.05–8.08 (m, 2 H). Anal. Calcd for $C_{41}H_{44}O_6$: C, 77.82; H, 7.01. Found: C, 77.98; H, 6.95.

(1α,4α,4aβ,4bα,4cβ,5α,5aβ,5bα,5cβ,6α,13α,13aβ,13bα,13cβ,14α,14aβ,14bα,14cβ)-1,4,4a,4c,5,5a,5c,6,13,13a,13c,14,14a,14c-Tetradecahydro-1,4:5,14:6,13-trimethano-7,12-dimethoxy-4b,5b,13b,14b-tetramethylbenzo[1⁗,2⁗:3⁗,4⁗]cyclobuta[1⁗,2⁗:3⁗,4⁗]cyclobuta[1⁗,2⁗:4″,5″]benzo[1″,2″:3′,4′]cyclobuta[1′,2′:3,4]cyclobuta[1,2-*b*]anthracene (8d(0,1)). To a solution of **8a(0,1)** (12.0 g, 19.0 mmol) in dry THF (200 mL), under a nitrogen atmosphere, was added $LiAlH_4$ (1.45 g, 35 mmol). The mixture was refluxed for 18 h. To the cooled reaction mixture was added successively water (2 mL), 15% aqueous NaOH (7 mL), and water (5 mL). The mixture was filtered, and the filtrate was evaporated under reduced pressure to give diol **8b(0,1)** (9.1 g, 83%) which was not purified further: IR (Nujol, cm^{-1}) 3250 (br, OH).

Methane sulfonyl chloride (3.67 g, 32 mmol) was added dropwise to a cooled (0 °C) solution of **8b(0,1)** (9.1 g, 15.8 mmol) in dry pyridine (100 mL). The resulting solution was maintained at −10 °C for 48 h after which it was poured onto crushed ice and then extracted with CH_2Cl_2 (3 × 200 mL). The organic extract was washed successively with aqueous 2 M HCl and aqueous $NaHCO_3$, then dried, and evaporated to give dimesylate **8c(0,1)** which was not purified. A stirred mixture of **8c(0,1)** (11.2 g, 15.3 mmol) and $LiAlH_4$ (1.16 g, 30.5 mmol) in dry THF (175 mL) was refluxed for 18 h. Use of the same workup procedure as described above for the synthesis of **8b(0,1)** gave, after recrystallization from MeOH **8d(0,1)** (6.5 g, 78%), mp 296 °C: ^{1}H NMR (300 MHz, $CDCl_3$) δ 0.79 (s, 6 H, 2 × CH_3), 0.96 (s, 6 H, 2 × CH_3), 1.11 (d, J = 9.2 Hz, 1 H), 1.32 (d, J = 9.2 Hz, 1 H), 1.56 (s, 2 H), 1.64 (br s, 2 H), 1.67 (d, J = 9.8 Hz, 1 H), 1.69 (s, 2 H), 1.87 (s, 2 H), 1.94 (d, J = 9.8 Hz, 1 H), 2.08 (s, 2 H), 2.16 (s, 2 H), 2.70 (t, J = 1.6 Hz, 2 H), 3.64 (br s, 2 H), 3.98 (s, 6 H, 2 × OCH_3), 5.97 (t, J = 1.9 Hz, 2 H), 7.41–7.44 (m, 2 H), 8.05–8.09 (m, 2 H). Anal. Calcd for $C_{39}H_{44}O_2$: C, 85.99; H, 8.14. Found: C, 86.11; H, 8.20.

(1α,4α,4aα,5β,5aα,5bβ,5cα,6β,6aα,6bβ,6cα,7β,14β,14aα,14bβ,14cα,15β,15aα,15bβ,15cα,16β,16aα)-1,2,3,4,4a,5,5a,5c,6,6a,6c,7,14,14a,14c,15,15a,15c,16,16a-Eicosahydro-1,4:5,16:6,15:7,14-tetramethano-8,13-dimethoxy-5b,6b,14b,15b-tetramethylnaphthol[2⁗⁗,3⁗⁗:3⁗⁗,4⁗⁗]cyclobuta[1⁗⁗,2⁗⁗:3⁗⁗,4⁗⁗]cyclobuta[1⁗⁗,2⁗⁗:4‴,5‴]benzo[1‴,2‴:3′,4′]cyclobuta[1′,2′:3,4]cyclobuta[1,2-*b*]anthracen-17-one 10(0,2) and the 17-Dicyanomethylene Derivative 1(12). A solution of **8d(0,1)** (4.2 g, 7.7 mmol) and **12** (4.0 g, 15.2 mmol) in *o*-xylene (50 mL) was refluxed for 5 days. Azeotropic removal of the xylene, through addition of ethanol (50 mL), gave a residue which was recrystallized from MeOH to give **9a(0,2)** (6 g, 96%), mp 295–296 °C: ^{1}H NMR (300 MHz, $CDCl_3$) δ 0.75 (s, 6 H, 2 × CH_3), 0.94 (s, 6 H, 2 × CH_3), 1.30 (d, J = 11.8 Hz, 1 H), 1.35 (d, J = 11.8 Hz, 1 H), 1.56 (d, J = 10.5 Hz, 1 H), 1.64 (d, J = 10.5 Hz, 1 H), 1.67 (d, J = 9.5 Hz, 1 H), 1.86 (s, 2 H), 1.87 (s, 2 H), 1.92 (d, J = 9.5 Hz, 1 H), 1.96 (s, 2 H), 2.02 (s, 2 H), 2.16 (s, 2 H), 2.18 (s, 2 H), 2.34 (s, 2 H), 3.49 (s, 3 H, OCH_3), 3.53 (s, 3 H, OCH_3), 3.63 (br s, 2 H), 3.98 (s, 6 H, 2 × OCH_3), 7.42–7.45 (m, 2 H), 8.06–8.09 (m, 2 H).

Sodium (20.0 g, 0.87 mmol) was added piecewise to a refluxing solution of **9a(0,2)** (6.0 g, 7.4 mmol) in THF (20 mL) and *i*-PrOH (150 mL). The resulting mixture was refluxed for 17 h and then worked up, as described above for the synthesis of **9b(0,0)**, to give a mixture of **9b(0,2)** and products resulting from the reduction of the naphthalene ring. Rearomatization with DDQ, as described for the synthesis of **9b(0,0)**, gave, after recrystallization from MeOH/acetone, **9b(0,2)** (2.6 g, 52%), which was not characterized further: partial ^{1}H NMR (60 MHz, $CDCl_3$) δ 0.73 (s, 6 H, 2 × CH_3), 0.97 (s, 6 H, 2 × CH_3), 3.03 (s, 3 H, OCH_3), 3.09 (s, 3 H, OCH_3), 3.60 (br s, 2 H), 3.97 (s, 6 H, 2 × OCH_3), 6.01 (m, 2 H), 7.40–7.65 (m, 2 H), 8.05–8.31 (m, 2 H).

9b(0,2) (2.5 g, 3.73 mmol) in EtOAc (80 mL) was hydrogenated at 1 atm and 25 °C by using 10% Pd/C (100 mg) until further uptake of H_2 had ceased. Standard workup procedure gave the 17,17-dimethylacetal of **10(0,2)** (2.3 g, 92%), mp 263–264 °C, whose ^{1}H NMR spectrum revealed complete absence of double bond.

A solution of the acetal of **10(0,2)** (0.5 g, 0.74 mmol) in formic acid (50 mL) and THF (5 mL) was stirred at 25 °C for 18 h. The formic acid was removed under reduced pressure, and the residue was recrystallized from EtOAc/acetone to give **10(0,2)** (0.4 g, 86%), mp 296–297 °C: IR (KBr, cm^{-1}) 1780 (C=O); ^{1}H NMR (300 MHz, $CDCl_3$) δ 0.80 (s, 6 H, 2 × CH_3), 0.94 (s, 6 H, 2 × CH_3), 1.57 (br s, 2 H), 1.63–1.75 (overlapping multiplets, 4 H), 1.83 (m, 2 H), 1.87 (br s, 4 H), 1.90–2.03 (overlapping multiplets, 6 H), 1.97 (s, 2 H), 2.03 (s, 2 H), 2.16 (s, 2 H), 2.21 (s, 2 H), 3.63 (br s, 2 H), 3.97 (s, 6 H, 2 × OCH_3), 7.41–7.45 (m,

(55) Ahmad, N.; Levison, J. J.; Robinson, S. D.; Uttley, M. F. *Inorg. Synth* **1974**, *15*, 45–64.

2 H), 8.05–8.09 (m, 2 H). Anal. Calcd for $C_{44}H_{50}O_3$: C, 84.30; H, 8.04. Found: C, 84.11; H, 7.77.

Dicyanomethylation of **10(0,2)** (0.25 g, 0.4 mmol) was carried out as described above for the synthesis of **1(6)**. Recrystallization from EtOAc gave **1(12)** (0.26 g, 96%), mp 225–226 °C: IR (KBr, cm^{-1}) 2242 (CN); ^1H NMR (300 MHz, $CDCl_3$) δ 0.79 (s, 6 H, 2 × CH_3), 0.94 (s, 6 H, 2 × CH_3), 1.55–1.68 (overlapping multiplets, 6 H), 1.75 (t, J = 2.1 Hz, 2 H), 1.84 (upfield half of partially obscured doublet, 1 H), 1.85 (s, 2 H), 1.87 (br s, 2 H), 1.90 (br s, 2 H), 1.93 (downfield half of partially obscured doublet, 1 H), 2.02 (d, J = 7.8 Hz, 1 H), 2.03 (s, 2 H), 2.06 (d, J = 7.8 Hz, 1 H), 2.16 (s, 2 H), 2.22 (s, 2 H), 2.96 (quintet, J = 2.1 Hz, 2 H), 3.62 (s, 2 H), 3.97 (s, 6 H, 2 × OCH_3), 7.42–7.45 (m, 2 H), 8.06–8.09 (m, 2 H). Anal. Calcd for $C_{47}H_{50}N_2O_2$: C, 83.64; H, 7.47; N, 4.15. Found: C, 83.35; H, 7.47, N, 3.98.

Measurements

Electrochemical measurements were performed by using a glassy carbon working electrode and an Ag/AgCl/KCl (saturated) reference electrode (−40 mV relative to the saturated calomel electrode (SCE)) in acetonitrile containing 0.1 M tetraethylammonium tetrafluoroborate as a supporting electrolyte. Static absorption and emission measurements were performed by using Hewlett-Packard 8451A and Spex Fluorolog instruments.

Fluorescence lifetimes have been obtained by time correlated single photon counting. The experimental setup is an improved version[56] of the one developed by de Vries et al.[57] Excitation pulses (7 ps fwhm) are created by synchronously pumping a Rh6G dye laser (Coherent 490 with extended cavity) with a mode-locked Ar^+ laser (Coherent CR8, repetition rate 94 MHz). The second harmonic of the dye laser is then generated by means of a 90° phase-matched ADA crystal, at exit of which the fundamental frequency is filtered off with a Schott UG5 filter. The wavelength of the UV pulses thus created was 303 nm.

(56) Bebelaar, D. *Rev. Sci. Instrum.* **1986**, *57*, 1116–1125.
(57) de Vries, J.; Bebelaar, D.; Langelaar, J. *Opt. Commun.* **1976**, *18*, 24–26.

Fluorescence of the samples was focussed onto the entrance slit of a Zeiss M20 monochromator by means of a quartz condensor and a Dove prism. Light detection was performed by means of a Hamamatsu R1564U-01 microchannel plate photomultiplier, with an optical time response of 47 ps at 273 nm.[56] The output of this photomultiplier was amplified by an ENI 500 LM amplifier. The amplified pulses were fed into a Tennelec 455 constant fraction discriminator producing the start pulses for a calibrated Ortec 457 time-to-amplitude-converter (TAC). Care was taken that the rate of start pulses did not exceed 10^{-4} of the laser repetition rate to ensure good statistics.

Stop pulses for the TAC were derived directly from the sync. output of the modelock driver. The output of the TAC (a voltage proportional to the time elapsed between start and stop pulse) was digitized and accumulated in an EG&G 918 multichannel buffer coupled to an IBM personal computer. The overall time response of the system was measured to be 70 ps fwhm by directly recording the stray light from a milky suspension of Al_2O_3 in water.

Recorded spectra were analyzed by means of a homewritten program based on iterative reconvolution. This allows for the presence of more than one exponential decay and automatically corrects for nonlinearity in the TAC time-base and for residual emission resulting from previous excitation pulses. The quality of a fit was judged from the normalized residuals and the χ^2, the latter being always smaller than 1.6. Realistic simulations have shown that this program is capable of determining lifetimes as short as 20 ps to within 5 ps accuracy.

Acknowledgment. We express our sincere thanks to Ing. D. Bebelaar and Dr. A. M. G. Kunst for their valuable contributions to the technical realization of the time-resolved emission measurements. The present investigations were supported by the Australian Research Grants Scheme and in part by the Netherlands Foundation for Chemical Research (SON) with the financial aid from the Netherlands Organization for the Advancement of Pure Research (ZWO).

On the Nature of Halogen Atom Transfer Reactions of $Re(CO_4)L^{\cdot}$ Radicals[1]

Kang-Wook Lee and Theodore L. Brown*

Contribution from the School of Chemical Sciences, University of Illinois at Urbana—Champaign, Urbana, Illinois 61801. *Received October 9, 1986*

Abstract: Rhenium carbonyl radicals $Re(CO)_4L^{\cdot}$ (L = $P(CH_3)_3$, $P(O\text{-}i\text{-}C_3H_7)_3$), generated by N_2 laser flash photolysis, react with organic halides in a bimolecular atom transfer reaction to form $XRe(CO)_4L$ (X = Cl, Br, I). Rate constants for reactions with 18 organic halogen atom donors were measured in toluene at 22 °C. The rate constants do not correlate well with available thermochemical C–X bond energies. Rate constants for bromine atom transfer for a series of benzyl bromides with $Re(CO)_4P(O\text{-}i\text{-}C_3H_7)_3^{\cdot}$ obey a Hammett equation correlation, with ρ = 0.75. The data are well-fitted by the Marcus/Agmon–Levine equation for atom or electron transfer, when the half-wave reduction potentials for the organic halides are employed as a measure of relative overall free energy change in the rate-determining process. The data are similarly well accommodated by the Rehm–Weller equation. The estimated intrinsic barriers, $\Delta G^{\ddagger}(0)$, are 3.5 kcal mol^{-1} for L = $P(CH_3)_3$ and 5.0 for L = $P(O\text{-}i\text{-}C_3H_7)_3$. The experimental results provide the first extensive test of the Marcus/Agmon–Levine or Rehm–Weller equation for halogen atom transfer. They suggest that atom transfer processes could be accommodated within such a theoretical framework when variations in electronic or steric properties are not so large as to markedly alter the equilibrium constant for formation of the encounter complex or the magnitude of the intrinsic barrier. They also provide an indication that electron transfer is a significant component in the reaction process and that configurational changes (C–X bond stretch and X–Re bond formation) in attaining the transition state are not large, or largely compensating.

Metal-centered radicals based on transition metal organometallic compounds have been the subject of much recent work.[2] Our interest has centered on metal carbonyl radicals. These can be produced by a variety of means, including atom abstraction,

0002-7863/87/1509-3269$01.50/0